



Reis, A. D. d., Scherer, C. M. d. S., Amarante, F. B. d., Rossetti, M. d. M. M., Kifumbi, C., de Souza, E. G., Ferronato, J. P. F. and Owen, A. (2019) Sedimentology of the proximal portion of a large-scale, Upper Jurassic fluvial-aeolian system in Paraná Basin, southwestern Gondwana. *Journal of South American Earth Sciences*, 95, 102248. (doi: [10.1016/j.jsames.2019.102248](https://doi.org/10.1016/j.jsames.2019.102248)).

This is the author's final accepted version.

There may be differences between this version and the published version. You are advised to consult the publisher's version if you wish to cite from it.

<http://eprints.gla.ac.uk/189616/>

Deposited on: 04 July 2019

Enlighten – Research publications by members of the University of Glasgow  
<http://eprints.gla.ac.uk>

# Accepted Manuscript

Sedimentology of the proximal portion of a large-scale, Upper Jurassic fluvial-aeolian system in Paraná Basin, southwestern Gondwana

Adriano Domingos dos Reis, Claiton Marlon dos Santos Scherer, Francyne Bochi do Amarante, Marcos de Magalhães May Rossetti, Carrel Kifumbi, Ezequiel Galvão de Souza, João Pedro Formolo Ferronato, Amanda Owen

PII: S0895-9811(18)30311-0

DOI: <https://doi.org/10.1016/j.jsames.2019.102248>

Article Number: 102248

Reference: SAMES 102248

To appear in: *Journal of South American Earth Sciences*

Received Date: 26 July 2018

Revised Date: 1 June 2019

Accepted Date: 24 June 2019

Please cite this article as: Reis, A.D.d., Scherer, C.M.d.S., Amarante, F.B.d., Rossetti, Marcos.de.Magalhã.May., Kifumbi, C., de Souza, Ezequiel.Galvã., Ferronato, Joã.Pedro.Formolo., Owen, A., Sedimentology of the proximal portion of a large-scale, Upper Jurassic fluvial-aeolian system in Paraná Basin, southwestern Gondwana, *Journal of South American Earth Sciences* (2019), doi: <https://doi.org/10.1016/j.jsames.2019.102248>.

This is a PDF file of an unedited manuscript that has been accepted for publication. As a service to our customers we are providing this early version of the manuscript. The manuscript will undergo copyediting, typesetting, and review of the resulting proof before it is published in its final form. Please note that during the production process errors may be discovered which could affect the content, and all legal disclaimers that apply to the journal pertain.



1 **Sedimentology of the proximal portion of a large-scale, Upper Jurassic fluvial-aeolian**  
2 **system in Paraná Basin, southwestern Gondwana**

3

4

5 Adriano Domingos dos Reis<sup>a,#</sup>

6 Claiton Marlon dos Santos Scherer<sup>b</sup>

7 Francyne Bochi do Amarante<sup>a</sup>

8 Marcos de Magalhães May Rossetti<sup>c</sup>

9 Carrel Kifumbi<sup>a</sup>

10 Ezequiel Galvão de Souza<sup>d</sup>

11 João Pedro Formolo Ferronato<sup>a</sup>

12 Amanda Owen<sup>e</sup>

13

14

15 <sup>a</sup> Programa de Pós-Graduação em Geociências, Universidade Federal do Rio Grande do Sul, Av.

16 Bento Gonçalves 9500, Prédio 43137, Agronomia; 91501-970 Porto Alegre, RS, Brazil

17 <sup>b</sup> Instituto de Geociências, Universidade Federal do Rio Grande do Sul, Brazil

18 <sup>c</sup> Department of Geology, University of Canterbury, New Zealand

19 <sup>d</sup> Universidade Federal do Pampa, Brazil

20 <sup>e</sup> University of Glasgow, United Kingdom

21 <sup>#</sup> Corresponding Author. Email: a\_d\_reis@hotmail.com

22

23

24

25

26

27

28

29

**Abstract**

Upper Jurassic sedimentary rocks of Guará Formation record the environmental and geotectonic changes of the early break-up stages in the southwestern portion of Gondwana. Newly-described occurrences of this formation allow the expansion of its areal distribution to the central part of the Paraná Basin, Brazil. Four vertical sections are presently described in Paraná State, Brazil. Nineteen lithofacies were grouped in five facies associations, through the classical method of facies analysis. The facies analysis included Guará Formation and the adjacent portions of the underlying Pirambóia Formation and the overlying Botucatu Formation. The depositional system of Pirambóia Formation was wet aeolian fluvial-influenced and is composed by aeolian dunes, aeolian sandsheets/interdunes and ephemeral fluvial deposits facies associations. The Guará Formation is composed of multistorey fluvial facies association constituting a highly amalgamated perennial fluvial system. It is overlaid by the Botucatu Formation, characterized as a dry aeolian system formed by aeolian dune deposits. The stratigraphic units are separated by regional unconformities marked by a shift in facies and depositional systems that reflect climatic changes. The Guará Formation depositional model, established in correlation with southern sections, represents a broad fluvial system with aeolian interaction deposited in a wide basin with more than 800 km in extension. This large depositional paleoenvironment, together with other Upper Jurassic records in southwestern Gondwana, represents the early rift stage of Gondwana break-up.

**Keywords:** Fluvial-aeolian interaction, braided fluvial, climatic changes, Upper Jurassic, southwestern Gondwana

51

**1. Introduction**

Understanding depositional systems are essential for palaeogeographic and palaeoclimatic reconstructions. The period between Late Jurassic and Early Cretaceous was marked by several palaeoenvironmental changes in Western Gondwana, promoted mainly by

56 tectonic processes of continental break-up and opening of the South Atlantic Ocean (Kuchle et  
57 al., 2011; Seton et al., 2012; Salomon et al., 2017). Sedimentary basins are an essential record to  
58 in understanding the palaeoenvironmental evolution of a particular area, and the Paraná Basin,  
59 due to its large extension and location around the forming South Atlantic rift, is a key laboratory  
60 to study such evolution.

61 In the last years, different studies have identified Upper Jurassic fluvial-aeolian deposits  
62 in the southern portion of Paraná Basin, encompassed in the Guará (southern Brazil) and  
63 Tacuarembó (Uruguay) Formations (Scherer and Lavina, 2005, 2006; Perea et al., 2009; Reis,  
64 2016; Amarante et al., 2019; Francischini et al. 2015). These formations represent the distal  
65 portion of a big distributive fluvial system that flowed to the southwest (Amarante et al., 2019).  
66 However, there are doubts about the extension of this system to the central part of the Paraná  
67 Basin, as well the possible facilogic variations in the proximal portions of the distributive  
68 system. We presently expand the areal distribution of the Guará Formation and evaluate the  
69 significance of this in terms of basin evolution inside the southwestern Gondwana context.

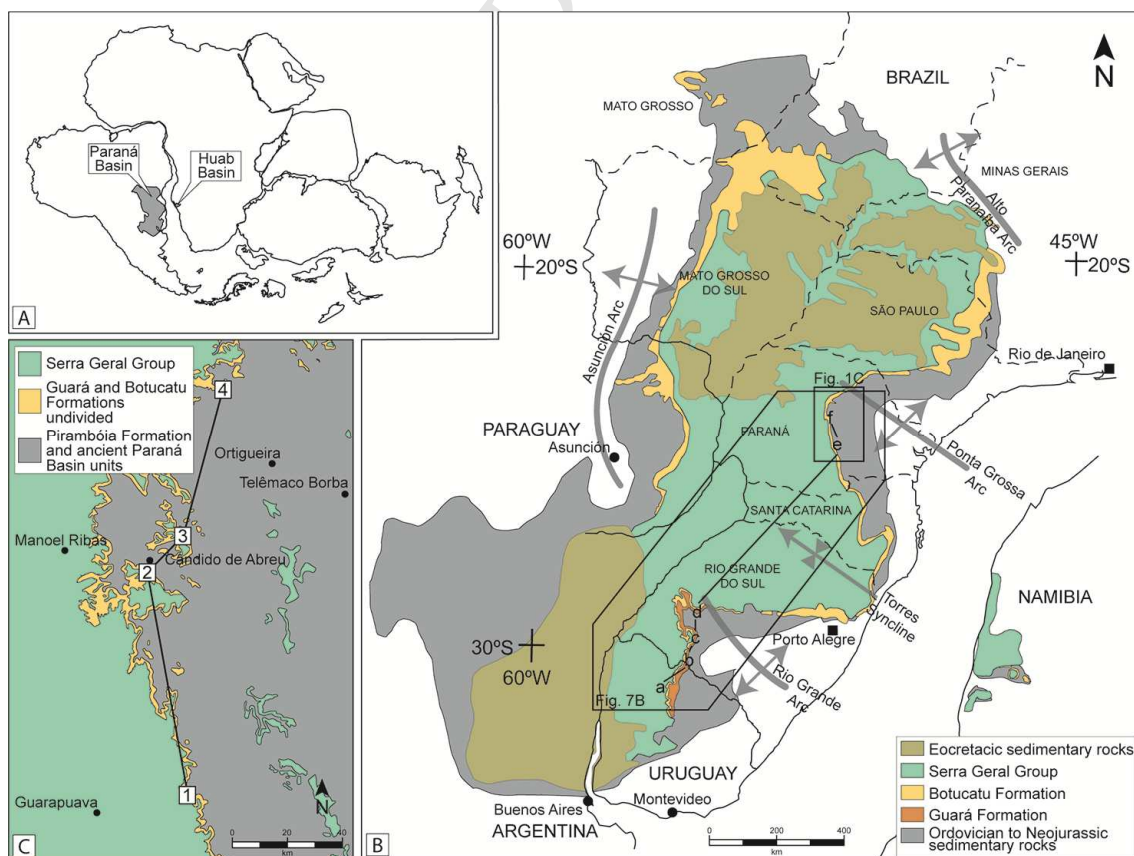
70 Facies analysis of four vertical profiles led to the identification of facies associations  
71 and depositional systems of Guará Formation, individualizing it from the adjacent Botucatu and  
72 Pirambóia Formations. Correlation of the profiles with previous occurrences allowed the  
73 establishment of Guará Formation as a record of a distinct paleoenvironmental and geotectonic  
74 setting in the evolution of Paraná Basin; a huge fluvial system interacting with aeolian systems  
75 in a wide endorheic basin.

76

## 77 **2. Geological Setting**

78 The Paraná Basin is an intracratonic basin covering an area of 1,400,000 km<sup>2</sup> across  
79 Brazil, Argentina, Uruguay, Paraguay with a small remnant Huab Basin in Namibia (Milani et  
80 al., 2007; Fig. 1A and B). The basin records various periods of subsidence and sedimentation  
81 from Ordovician to Cretaceous (Milani, 1997; Milani et al., 1998, 2007). The Paleozoic basin  
82 fill was constructed by three second-order transgressive-regressive cycles (Milani, 1997; Milani

83 et al., 1998, 2007). The Mesozoic record is composed of continental successions that comprise  
 84 six lithostratigraphic units bounded by regional unconformities (Milani, 1997; Scherer et al.,  
 85 2000; Fig. 2): (1) Sanga do Cabral Formation (Scitian), consisting of fluvial, lacustrine and  
 86 aeolian deposits; (2) Santa Maria and Caturrita Formation (Ladinian to Norian) composed of  
 87 fluvial-lacustrine deposits; (3) Mata Sandstone (Norian) deposits of braided fluvial system; (4)  
 88 Guar Formation (Upper Jurassic), constituted by fluvial and fluvial-aeolian systems; (5)  
 89 Botucatu Formation (Lower Cretaceous), recording dunes of dry aeolian system fossilized under  
 90 the Serra Geral Formation volcanic lavas; and (6) Bauru Group (Upper Cretaceous) composed  
 91 of fluvial and aeolian deposits. The Piramb Formation occurs in the northwestern portion of  
 92 the basin, with fluvial-aeolian deposits of undetermined age, possibly Permian to Eocretaceous  
 93 (Giannini et al., 2004). The unconformities are related to active margin tectonics of  
 94 southwestern Gondwana and to South Atlantic rifting process (Milani, 1997; Zeffass et al.,  
 95 2003, 2004). These tectonic events activated and reactivated the NW-SE, NE-SW and E-W fault  
 96 systems, main drivers of sedimentation and preservation of stratigraphic units (Milani, 1997;  
 97 Milani et al., 1998, 2007; Quintas et al., 1999; Zeffass et al., 2004, 2005).



98

99 **Figure 1.** Location of the studied area and correlated sections in the contexts of Paraná Basin  
 100 and Gondwana. A) Paraná Basin and its counterpart in southwestern Africa Huab Basin,  
 101 positioned in Upper Jurassic Gondwana (based on Schmitt and Romeiro, 2017). B) Paraná and  
 102 Huab Basins locations. The original occurrence of Guará Formation is in orange (small letters a,  
 103 b, c and d). The newly discovered occurrences of Guará Formation are in the area with the letters  
 104 f and e, highlighted in Fig. 1C (Modified from Zalán et al., 1987; Scherer and Lavina 2005,  
 105 2006; Scherer and Goldberg, 2007; Amarante 2017; Rossetti et al., 2017) C) Study area in  
 106 central Paraná state, the numbers (1 to 4) are the logged sections where Guará Formation was  
 107 recognized in this work..

		SW		NE
		Uruguay (from Perea et al., 2009)	Rio Grande do Sul State, Brazil (modified from Milani, 1997; Scherer et al., 2000)	Paraná State, Brazil (this study, based in Milani et al., 2007)
Cretaceous	Upper			Bauru Gr.
	Lower			
Jurassic	Upper	Arapey Fm. Takuarembó Fm.	Serra Geral Gr. Botucatu Fm.	Serra Geral Gr. Botucatu Fm.
	Middle			
	Lower			
Triassic	Upper		Mata Sandstone	Pirambóia Fm. (unknown age)
	Middle		Caturrita Fm.	
	Lower		Santa Maria Fm.	
Permian		Buena Vista Fm.	Sanga do Cabral Fm. / Rio do Rasto Fm.	Rio do Rasto Fm.

\*previously described as "torrential facies" of Botucatu Fm. by Soares (1975)

108  
 109 **Figure 2.** Stratigraphy of southern to central portions of Paraná Basin, from Upper Permian to  
 110 Mesozoic, highlighting the stratigraphic position of Guará and Botucatu Formations, and the  
 111 controversial age of Pirambóia Formation. Modified from Soares (1975), Milani (1997), Scherer  
 112 et al. (2000), Milani et al. (2007) and Perea et al. (2009). SW - southwest; NE - northeast; Gr. -  
 113 Group; Fm. - Formation; Mb. - Member.

114 The Pirambóia Formation is recognized in the study area as dunes and wet interdunes.  
 115 Despite extensive and inconclusive discussion about nomenclature, age and areal distribution of  
 116 Pirambóia Formation (Francischini et al., 2018), this work is restricted to the unit's definition on  
 117 the study area, in Paraná States (Fig. 2). Firstly described by Pacheco (1927), the Pirambóia  
 118 Formation was later detailed (Soares et al., 1973; Soares, 1975), allowing the recognition of an  
 119 erosive unconformity between Pirambóia Formation and overlying Lower Cretaceous Botucatu  
 120 Formation. Modern sedimentological concepts demonstrate that the Pirambóia Formation

121 consists of aeolian dunes, wet and dry interdunes and ephemeral fluvial (wadis) deposits,  
122 composing a fluvial-aeolian system (Wu and Caetano-Chang, 1992; Caetano-Chang and Wu,  
123 1994).

124 The Lower Cretaceous Botucatu Formation is considered a record of a palaeodesert that  
125 covered an area of more than 1,500,000 km<sup>2</sup> (Bigarella and Salamuni, 1961; Scherer and  
126 Goldberg, 2007), cropping out in the edges of Paraná Basin in Brazil, Uruguay, Argentina,  
127 Paraguay, and has correlative deposits in Namibia (e.g. Twyfelfontein Formation; Stanistreet  
128 and Stollhoffen, 1999; Fig. 1). Morphological reconstructions of aeolian dunes Performed in  
129 Botucatu Formation in southern Brazil demonstrated the occurrence of simple to compound  
130 crescentic aeolian dunes and complex linear draas (Scherer, 2000, 2002). Conglomerates and  
131 gravelly sandstones occur above its basal contact, brought by ephemeral streams (Bigarella and  
132 Salamuni, 1961; Soares, 1975; Almeida and Melo, 1981; Scherer, 2002). Soares (1975)  
133 identified, in his Paraná State study area, a package of sandstones with fluvial origin overlain by  
134 aeolian dunes which he termed the “torrential facies” of the Botucatu Formation. These fluvial  
135 deposits are the main focus of our study, in which we present a different origin for them, as part  
136 of Guará Formation. Despite this, Botucatu Formation deposits are considered a dry aeolian  
137 system developed in a hyper-arid climate (Scherer and Lavina, 2006). The upper boundary of  
138 the unit is overlain by volcanic rocks of Serra Geral Group which are concordant and  
139 transitional, as indicated by the preservation of features of interactions between the lava flows  
140 and active aeolian dunes, as impressions of lava lobes in the entirely preserved topset of dunes,  
141 recording their whole morphologies under lava-flows (Scherer, 2002; Waichel et al., 2008). Due  
142 to absence of internal hiatuses in the aeolian succession (supersurfaces, Scherer, 2002) and the  
143 intimate relation between aeolian sandstones and lava-flows, the age of Botucatu Formation is  
144 close to the beginning of Serra Geral Group magmatism, dated between 134.1 and 134.8 Ma  
145 (Valanginian; Renne et al., 1992; Thiede and Vasconcelos, 2010; Rossetti et al., 2017).

146 Upper Jurassic rocks in Paraná Basin were recorded in Uruguay, where it is known as  
147 the Batoví Member of Tacuarembó Formation (Perea et al., 2009) and in its counterpart, the  
148 Guará Formation in the Rio Grande do Sul State, southern Brazil (Scherer and Lavina, 2005,



149 Fig. 1). The relative ages are attributed to their respective fossil and ichnofossil assemblages  
150 (Scherer and Lavina, 2005; Perea et al., 2009; Francischini et al., 2015). The Batoví Member is  
151 a fluvial-aeolian system (Perea et al., 2009) composed by five facies associations: aeolian dunes,  
152 aeolian sandsheets, ephemeral fluvial channels, perennial braided fluvial channels and distal  
153 sheetfloods (Amarante et al., 2019). The paleocurrent pattern indicates paleowinds to the ENE,  
154 and fluvial paleoflows to the SSW (Amarante et al., 2019). The Guar Formation consists of  
155 fluvial (in its proximal northern portion) and fluvial-aeolian (in its distal southern portion)  
156 depositional systems, forming wetting-upward cycles (Scherer and Lavina, 2005). Paleocurrents  
157 of aeolian dunes in Guar Formation were to the NE and the fluvial paleocurrents were to the  
158 SSW (Scherer and Lavina, 2005).

159

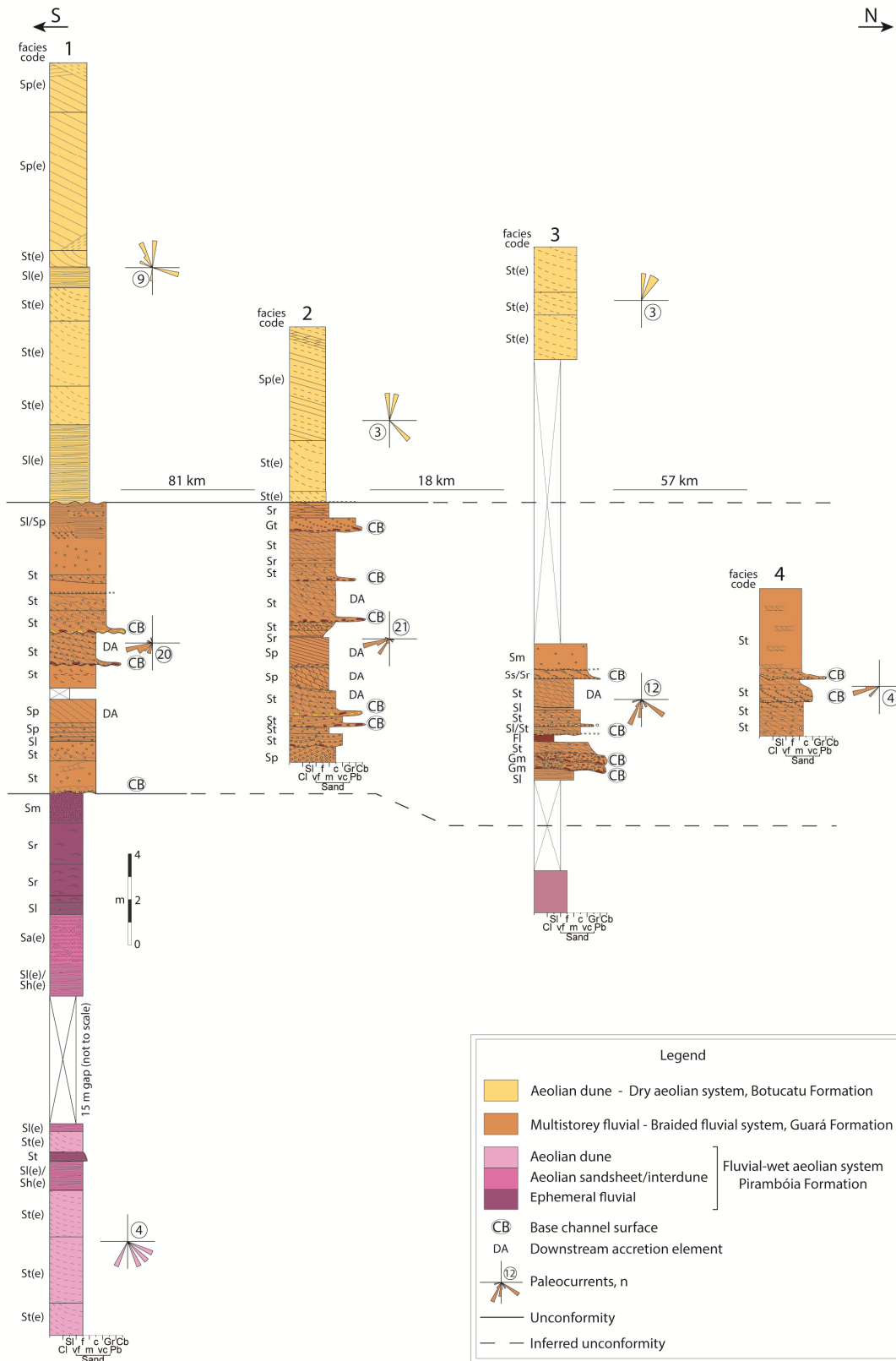
### 160 3. Methods

161 The Guar Formation crops out along escarpments that cross the central part of Paran  
162 State in Brazil. The locations to study are identified looking for places where this escarpment  
163 are cut by roads, quarries or rivers, spots in which the vegetation cover was opened. Four  
164 outcrops distributed along an N-S belt in (Fig. 1B and C, Fig. 3) are logged in vertical sections.  
165 Section 1 (2519'27" S; 5111'43" W) is from vertical road cuts at kilometre 290 of BR-373  
166 road, on the limit between Guarapuava and Prudentpolis municipalities. Section 2 (2436'37"  
167 S; 5120'59" W) is located 3 km to the south of Cndido de Abreu town, along a dirt road.  
168 Section 3 (2429'24" S; 5113'21" W) is situated 15 km to the northeast of Cndido de Abreu  
169 town, along a dirt road. Section 4 (2359'50" S; 5105'33" W) is located next to BR 373  
170 between Mau da Serra and Ortigueira, inside a farm.

171 Four vertical sections were constructed at a 1:50 scale, totalizing 88 m of rock  
172 succession (Fig. 3). Sedimentological data collected were classified with traditional methods of  
173 facies analysis (*sensu* Walker, 1992), in which the genetically-related lithofacies define facies  
174 associations corresponding to subenvironments within a depositional system. Lithofacies were  
175 codified by the principles of Miall (1977): the first capital letter represents the grain-size (G for

176 gravel, S for and F for fine sediments, i.e. mud) and the second lower case letter indicates  
177 sedimentary structure. Letter (e) was used to distinguish facies formed by aeolian processes.  
178 Measures of dip azimuths of foresets present in cross-bedded sandstone sets indicate  
179 paleocurrent orientations.

ACCEPTED MANUSCRIPT



180

181 **Figure 3.** Logged vertical sections, divided by facies associations, depositional systems and

182 stratigraphic units.. See Figure 1 for the location of logs. See Table 1 for facies code. The

183 Piramb Formation show a diversity of aeolian facies associations and paleocurrents pattern to

184 S. There is a 15 m gap on the logged section of Pirambóia Formation is Section 1 due to  
185 vegetation covering the outcrop. The Guará Formation is between two regional unconformities,  
186 showing a series of amalgamated channels with paleoflow to SW in all the 3 sections. Botucatu  
187 Formation, constituted by aeolian dunes, show a variable range of paleocurrents. Where the  
188 unconformity surface was covered by vegetation, the surface is a dashed line and the top and  
189 base of Guará Formation is estimated.

#### 190 **4. Lithofacies**

191 Here we present a brief summary of the general composition and texture of the  
192 sediments in each Formation recorded. Are stated here only features observable in macroscopic  
193 analysis in the field. The detailed descriptions and interpretations of each lithofacies are in  
194 Table 1.

195 The Pirambóia Formation succession presents a variety of lithofacies formed by  
196 subaqueous and wind-related processes (Fig. 3, Table 1). The macroscopic analysis in samples  
197 identified fine-grained sandstones with quartz and feldspar, indicating arkosic to sub-arkosic  
198 composition. The presence of argillaceous white material is notable, probably a diagenetic  
199 product. Sorting varies from well-sorted in the aeolian facies to poorly-sorted in subaqueous  
200 facies and the grains are well-rounded in general.

201 Lithofacies identified in Guará Formation are mainly cross-stratified medium- to very  
202 coarse-grained sandstones (rarely fine-grained), gravelly sandstones and conglomerates (Fig. 3,  
203 Table 1). Sand is poorly to very poorly-sorted with subrounded to rounded grains. The gravel  
204 fraction varies from rounded to subangular – normally the quartz clasts are more rounded while  
205 the mud clasts and lithoclasts are subrounded to subangular. Concerning the detrital  
206 composition, the sandstones and conglomerates of Guará Formation are very homogeneous.  
207 They are basically quartzarenites in sand fraction, while the gravel fraction is composed by  
208 quartz (granules to pebbles), mud clasts (granules to boulders) and sedimentary lithoclasts  
209 (pebbles to boulders). The presence of sedimentary lithoclasts is notable in gravel fraction, as it  
210 is composed of fine- to medium-grained sandstone clasts varying from pebble to boulder size

211 classes (Fig. 4D and E, Fig. 5C and D), and granule to boulder-sized mud clasts (Fig. 4D). Fine  
 212 sediments are restricted to mud clasts and one occurrence of laminated mudstone in Section 3  
 213 (Fig. 3).

214 Lithofacies of Botucatu Formation are sandstones deposited by aeolian processes,  
 215 homogeneous in composition and texture (Table 1). They are basically fine- to medium-grained  
 216 sub-arkosic sandstones, well-sorted and well-rounded sandstones.

217 **Table 1.** Summary of lithofacies, with description and interpretation of the forming process of  
 218 each lithofacies. The Lithofacies are grouped by stratigraphic unit (e.g., Pirambóia, Guará and  
 219 Botucatu Formations).

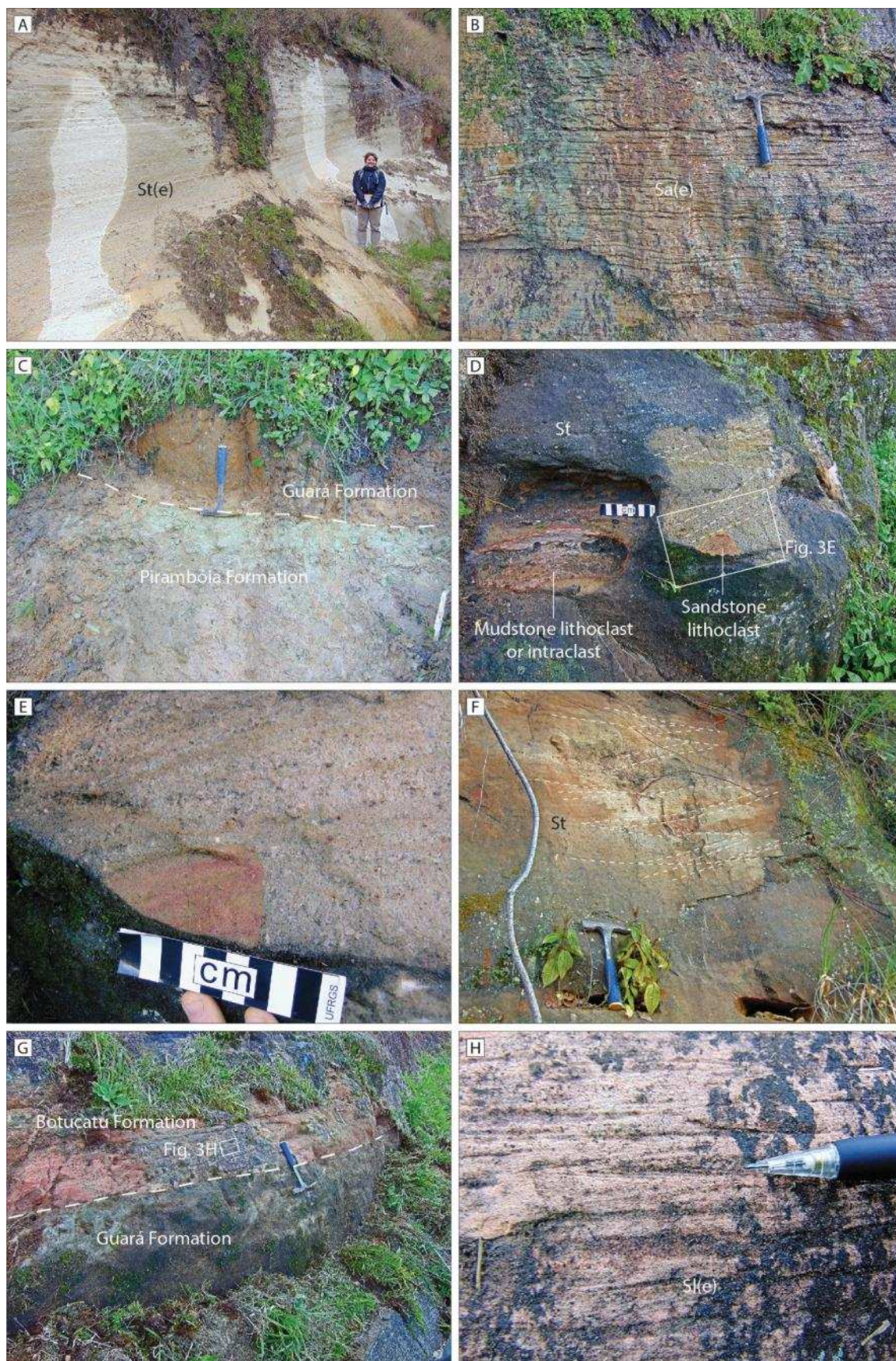
Code	Description	Interpretation
Pirambóia Formation		
St(e)	Fine-grained sandstones, well-sorted, trough cross-stratified in large scale sets (1.4-3.0 m thick, Fig. 4A). Foresets formed by millimetric pin stripe inversely-graded lamination.	Sinuuous-crested (3D) aeolian dunes alternating grainflow and translantent subcritical wind ripple migration in the lee side (Hunter, 1977; Hunter and Rubin, 1983).
Sl(e)/S(h)	Fine-grained sandstone, well-sorted, horizontal to low-angle lamination formed by thin pinstripe inversely graded laminae.	Translantent subcritical wind ripple migration over a plane to quasi-plane surface (Kocurek, 1981).
Sa(e)	Fine-grained sandstone, well-sorted, with crenulated plane-parallel lamination (Fig. 4B).	Adhesion structures originated by adherence of dry sand grains that were carried by wind over wet surfaces (Kocurek, 1981; Kocurek and Fielder, 1982).
St	Fine- to medium-grained sandstone, moderately-sorted, in normal graded trough cross-stratified sets.	Migration of subaqueous sinuous-crested dunes in unidirectional flow (Allen 1963; Miall, 1977; Collinson et al, 2006).
Sr	Fine-grained sandstone, poorly-sorted, with ripple cross-lamination	Migration of unidirectional subaqueous ripples with subcritical climbing angle (Allen, 1963; Miall, 1977).
Sl	Fine-grained sandstone, poorly-sorted, low-angle cross-stratified.	Structures formed in unconfined high energy flows, in transitional flow regime between upper and lower (Harms et al., 1982; Bridge and Best, 1988).
Sm	Fine-grained massive sandstone, moderately-sorted.	Fast deposition of subaqueous unidirectional high energy flow, hyper-concentrated in sediments, fluidization or intensive bioturbation (Miall, 1978, 1996)

## Guará Formation

Gt	The clast-supported sandy conglomerate, quartz pebbles, trough cross-bedded. Green muddy cobbles at the set base.	Migration of subaqueous sinuous-crested gravel dunes in unidirectional flow (Todd, 1996).
Gm	The clast-supported conglomerate, pebble-sized quartz clasts, reddish muddy intraclasts and sandstone lithoclasts cobble to boulder-sized, massive (Fig. 6B). Frequently at the base of cross-strata sets. Resting upon erosive surfaces, filling scours.	Deposition of bedload as diffuse gravel sheets (Hein and Walker, 1997) in the channel bottom, resulting from erosion of previous gravelly sands (quartz pebbles), overbank deposits (mud clasts) and ancient sedimentary rocks (sandstone lithoclasts).
Sm	Very coarse-grained sandstone, massive. Muddy pebbles at the bed bottom.	Fast deposition of subaqueous unidirectional high energy flow, hyper-concentrated (Scherer et al., 2015) in sediments, fluidization or intensive bioturbation (Miall, 1978, 1996).
St	Medium to very coarse-grained gravelly sandstone, trough cross-stratified (Fig. 4D and F, 5B and E, 6C, E and F). Sets varying from 10-20 up to 40 cm thick. Foresets and sets normally graded. Quartz and muddy granules and pebbles dispersive, at the set base and marking the foresets. Frequently deposited above Gm facies bed. Compound cosets with set bases gently inclined downstream. Cosets and sets with plane or concave base.	Migration of subaqueous sinuous-crested dunes in unidirectional flow (Allen 1963; Miall, 1977; Collinson et al, 2006). Compound downstream accretion elements of mid-channel bars (Allen, 1983; Haszeldine, 1983; Wizevich, 1992; Miall, 1996).
Sp	Medium to coarse-grained sandstone, planar cross-stratified. Dispersive quartz granules. Mudclasts and quartz granules and pebbles at the set base. Sets varying from 10-20 up to 40 cm thick. Simple large scale sets (up to 1.25 m). Compound cosets with set bases gently inclined downstream.	Migration of subaqueous straight-crested dunes in unidirectional flow (Allen 1963; Miall, 1977; Collinson et al, 2006). Simple and compound downstream accretion elements of mid-channel bars (Allen, 1983; Haszeldine, 1983; Wizevich, 1992; Bridge, 1993; Miall, 1996; Jo and Choug, 2001).
Sl	Medium to coarse-grained sandstone, moderately to poorly-sorted, low-angle cross stratification, alternated with facies St (Fig. 6B and D).	Structures formed in transitional flow between subcritical and supercritical (Harms et al., 1982; Bridge and Best, 1988).
Sr	Fine to coarse sandstones with ripple cross-lamination (Fig. 5E and F).	Migration of unidirectional subaqueous 2D or 3D in lower flow regime (Allen, 1963; Miall, 1977).
Ss	Very coarse-grained sandstone with sigmoidal cross stratification.	Migration of subaqueous dunes with rapid aggradation combining traction and suspension in lower- to upper-flow regime (Wizevich, 1992).
Fl	Gray-purple, laminated mudstone (Fig. 6D).	Deposition of suspended load by settling in standing water (Miall, 1977; Turner, 1980; Jo and Chough, 2001).

## Botucatu Formation

St(e)	Fine- to medium-grained sandstone, moderately to well-sorted, trough cross-stratified in large scale sets (0.8-6 m thick, Fig. 5F and G) formed by inversely graded foresets with millimetric pin stripe lamination or massive strata (1.5 cm thick).	Sinuuous-crested (3D) aeolian dunes, alternating grainflow and translantent subcritical wind ripple migration in the lee side (Hunter, 1977; Hunter and Rubin, 1983).
Sp(e)	Fine- to medium-grained sandstone, moderately to well-sorted, trough cross-stratified in large scale sets (2-6 m thick) formed by inversely graded foresets formed by millimetric pin stripe lamination or massive strata (1.5 cm thick).	Straight-crested (2D) aeolian dunes alternating grainflow and translantent subcritical wind ripple migration in the lee side (Hunter, 1977; Hunter and Rubin, 1983).
Sl(e)	Fine- to medium-grained sandstone, well-sorted, low-angle lamination formed by millimetric pin stripe inversely graded laminae (Fig. 4H).	Translantent subcritical wind ripple migration over a quasi-plane surface (Kocurek, 1981).



221

222

223

**Figure 4.** Details of Section 1 (Fig. 3). See Table 1 for facies code. A) Large scale cross strata of aeolian dune (facies St(e); person for scale 1.65 m high) and B) plane-parallel crenulated



224 adhesion structures (facies Sa(e); hammer length = 28 cm) from Pirambóia Formation. C) Sharp  
225 bounding surface (dashed line) marking the unconformity between Pirambóia and Guará  
226 Formations. D) Very coarse-grained cross-stratified sandstone (facies St, white dashed lines),  
227 with mudstone lithoclast or intraclast (limited by the red dashed line) and sandstone lithoclast  
228 (limited by the yellow dashed line) at the over an erosive surface representing the base of a  
229 fluvial channel. Each white or black bar on the scale has 1 cm. E) Detail of a medium-grained  
230 sandstone lithoclast at the base of a channel. F) Composite coset of trough cross stratification  
231 (facies St) compounding a downstream accretion element (DA). White dashed lines highlighting  
232 the sets and foresets. G) Sharp bounding surface (white dashed line) on the unconformity  
233 between Guará and Botucatu Formations. H) Detail of translent wind ripple lamination (facies  
234 Sl(e); pencil tip = 2 cm).

235

## 236 5. Facies Associations

### 237 5.1. Pirambóia Formation

#### 238 5.1.1. Aeolian dune facies association

239 This facies association comprises fine-grained, well-sorted, white sandstones that form  
240 large scale trough cross-stratified sets (St(e), Fig. 3, Section 1, Fig. 4A). Set thickness varies  
241 from 0.8 m to 3.0 m, and length around 2 m in outcrop, superimposed or in abrupt contact with  
242 aeolian sandsheet and ephemeral fluvial deposits. The stratification of foresets is constituted by  
243 millimetric laminae that exhibit an upward change from very fine- to fine-grained sandstone  
244 defining inverse grading, formed by the migration of translent subcritical wind ripples. The  
245 measured azimuths of foresets indicate palaeowind to SSE (as show the rose diagram in Fig. 3).

#### 246 Interpretation

247 Well-sorted, fine-grained sandstones arranged in large scale trough cross-stratified sets  
248 composed of wind ripple lamination suggest aeolian dune deposits (Hunter 1977, Kocurek,  
249 1991, Scherer et al. 2007). The exclusive presence of wind ripple lamination may represent: (a)  
250 a severely truncated dune set, where the lee slipface is not preserved; (b) a dune type or portion  
251 of the dune where the slipface is absent; or (c) a low relief dune without slipface (Kocurek,  
252 1991).

253

## 254 5.1.2. Aeolian sandsheet/interdune facies association

255 This facies association comprises fine-grained well-sorted white sandstones arranged  
256 into two distinct structures (Fig. 3, section 1): (1) Low-angle to horizontal millimetric  
257 lamination (Sl(e)/Sh(e)), with inversely graded laminae, formed by migration of translantent  
258 subcritical wind ripples over a plane or quasi-plane surface; (2) crenulated plane-parallel  
259 lamination (Sa(e); Fig. 4B) originated by adhesion of dry sand transported by wind in a wet  
260 substrate. The upward transition from facies Sl(e)/Sh(e) to Sa(e) is gradual. These facies are  
261 disposed in tabular packages 0.4 m to 1.4 m thick when in abrupt contact with aeolian dune  
262 facies association, or in thicker packages (4.6 m), directly in contact with ephemeral fluvial  
263 deposits.

## 264 Interpretation

265 Tabular packages of wind ripples and adhesion structures are characteristic of deposits  
266 of aeolian origin (Kocurek and Nielson, 1986; Clemmensen and Dam, 1993; Chakraborty and  
267 Chakraborty, 2001; Scherer and Lavina, 2005). The low-angle to horizontal wind ripple  
268 lamination was generated when dry sand was not sufficiently available for aeolian dune  
269 formation (Kocurek and Nielson, 1986; Clemmensen and Dam, 1993). The high water table  
270 intercepting the depositional surface is a significant mechanism that restricts dry sand supply  
271 (Kocurek and Nielson, 1986). Presence of adhesion structures testifies a moisturized substrate.  
272 Capillarity moisture was responsible for “freezing” and preserving wind ripple lamination  
273 (Kocurek and Nielson, 1986). In the Pirambóia sedimentary succession, there is a gradual  
274 transition from low-angle/horizontal wind ripple lamination to adhesion lamination, suggesting  
275 an increase in the humidity and local rise of the water table (Fig. 3, Section 1).

276 Tabular packages with horizontal lamination of aeolian origin can be formed in two  
277 different depositional settings: (a) metasaturated interdune areas located between aeolian dunes  
278 (e.g. Herries, 1993; Mountney & Thompson, 2002; Uličný, 2004); or (b) aeolian sandsheets, in  
279 context of low dry sand availability, inhibiting the construction of aeolian dunes (e.g. Trewin,  
280 1993; Veiga et al., 2002; Biswas, 2005). For Pirambóia Formation deposits, both interpretations

281 are possible. Horizontally-laminated aeolian deposits occur separating dune deposits and  
282 isolated between ephemeral fluvial deposits (Fig. 3, Section 1).

283 The interference of fluvial deposition in an aeolian system is also an important  
284 mechanism that controls dry sand supply (Kocurek and Nielson, 1986). Pirambóia Formation  
285 deposits present an interaction between ephemeral fluvial deposits and aeolian deposits, which  
286 indicates that fluvial activity has critical importance in the generation of aeolian sand sheets  
287 (Clemmensen and Dam, 1993; Chakraborty and Chakraborty, 2001; Scherer and Lavina, 2005).

288

### 289 5.1.3. Ephemeral fluvial deposits facies association

290 These deposits congregate facies resulting from subaqueous processes. Fine- and fine-  
291 to medium-grained white sandstone, moderately- to poorly-sorted, represents the main lithology  
292 (Fig. 3, section 1). The most recurrent structure in these deposits is subaqueous ripple  
293 lamination (Sr) arranged in a 3.6 m thick bed. Low-angle lamination formed in transitional flow  
294 (Sl) and massive (Sm) sandstones also occur. These facies together constitute a tabular  
295 sandbody 5 m thick, succeeding an aeolian sandsheet deposit, with sharp abrupt contact (Fig. 3,  
296 Section 1). In an alternative context, a single normal graded trough cross-bedded sandstone bed,  
297 representing a 3D subaqueous dune, occurs over an aeolian sandsheet deposit, with an erosive  
298 contact, and preceding aeolian dune strata (Fig. 3, Section 1).

### 299 Interpretation

300 Moderately to poorly-sorted sandstones displaying ripple lamination, low-angle cross-  
301 stratification, trough-cross stratification and massive structure suggest fluvial deposition in a  
302 highly variable energy flow context. Massive sandstones are generated by deposition under  
303 upper flow regime conditions hyper-concentrated in sediments (Miall, 1978, 1996). Low-angle  
304 cross-stratification represents accelerant or waning flow within a transitional stage between  
305 subcritical and supercritical flow regimes (Harms et al., 1982; Bridge and Best, 1988). On the  
306 other hand, ripple lamination and subaqueous 3D dunes can also be products of unidirectional  
307 current under lower flow regime conditions (Allen 1963; Miall, 1977; Collinson et al, 2006).  
308 Such variation in flow energy suggests deposition in poorly-confined to unconfined ephemeral

309 streams. The relationship of these deposits with aeolian sheets and aeolian dunes demonstrates  
310 fluvial-aeolian interactions, where fluvial transport and deposition invade the interdune area or  
311 cover aeolian sandsheets in periods of flash discharge, possibly at the border of aeolian system  
312 (Langford & Chan, 1989; Mountney and Jagger, 2004; Scherer and Lavina, 2005).

313

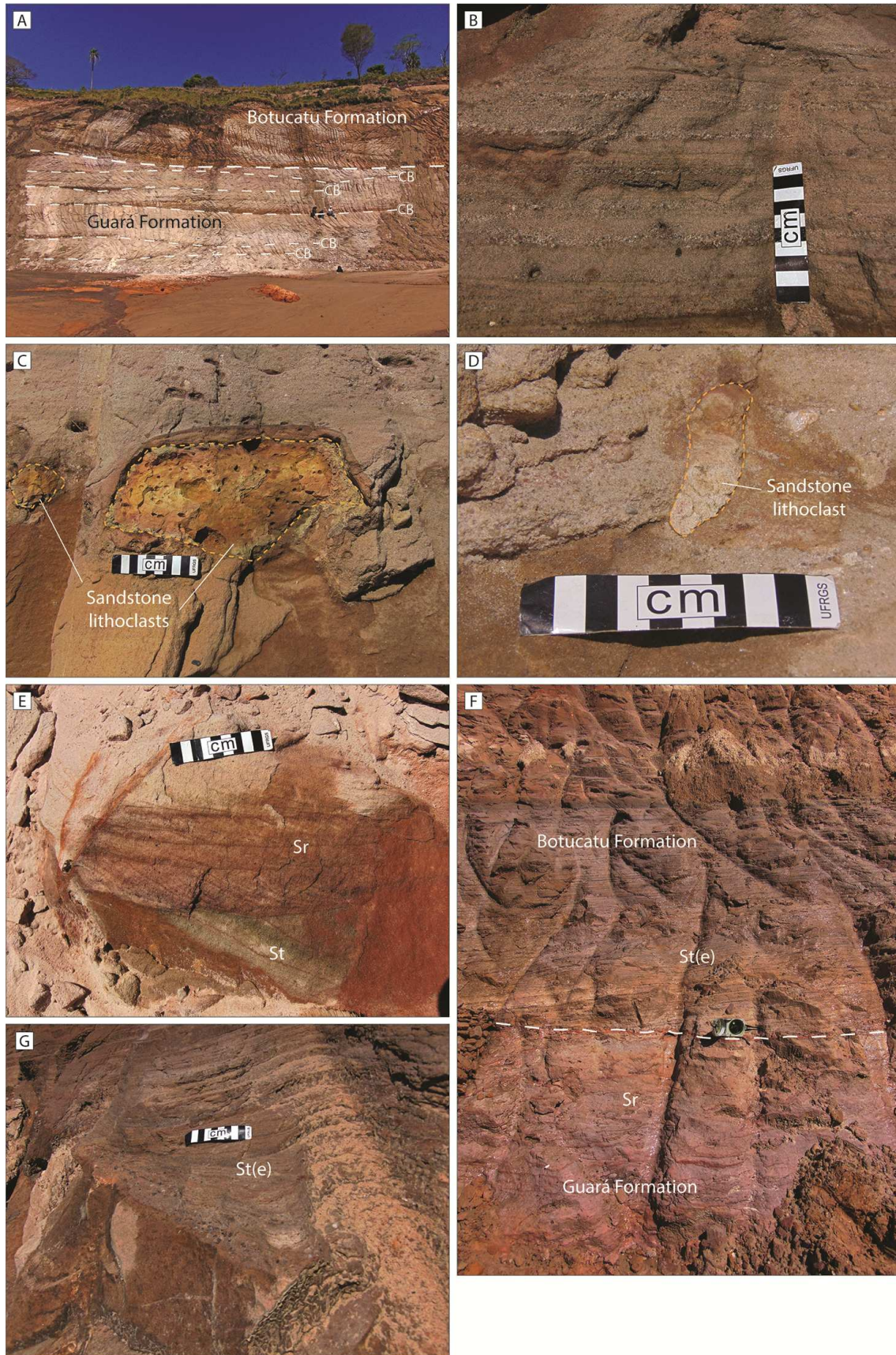
## 314 5.2. *Guará Formation*

### 315 5.2.1. Multistorey fluvial facies association

316 The deposits of Guará Formation are significantly composed of lithofacies that  
317 represent dune migration (e.g. St and Sp isolated sets; Fig. 3, Fig. 4D, 6C and E) and bedload or  
318 residual deposits that are deposited upon erosive surfaces (i.e. Gm; Fig. 3, Fig. 4D, E and F).  
319 Simple and compound elements such as downstream accretion (DA, Fig. 3, 6F) are represented  
320 by large scale (0.8 to 1.9 m thick) cross-stratified sets and cosets (Sp and St). In compound  
321 elements, individual sets are bounded by low-angle inclined surfaces, dipping in the same  
322 direction of the intraset cross strata (Fig. 4F, Fig. 6F). In general, these facies are organized as  
323 fining upwards packages with massive conglomerates (facies Gm) at the base, composed by  
324 pebble to boulder sandstone clasts, granule to boulder mud clasts and granule to pebble quartz  
325 grains. The packages rest upon sharp erosive surfaces overlain by cross-stratified sets and cosets  
326 (Fig. 3, Fig. 4D, Fig. 5A, C and D, Fig. 6B). Foresets and cross-strata sets are commonly  
327 normally graded, with quartz granules and pebbles dispersive or marking the foresets and set  
328 bases (Fig. 5B).

329 Other sandstone lithofacies have very subordinated occurrence, including low-angle  
330 cross stratified sets (Sl), subaqueous ripple cross lamination (Sr; Fig. 5E), sigmoidal cross-  
331 stratified sets (Ss) and massive sandstones (Sm). The minor record of fine lithofacies (Fl)  
332 deserves special attention (Fig. 6D).

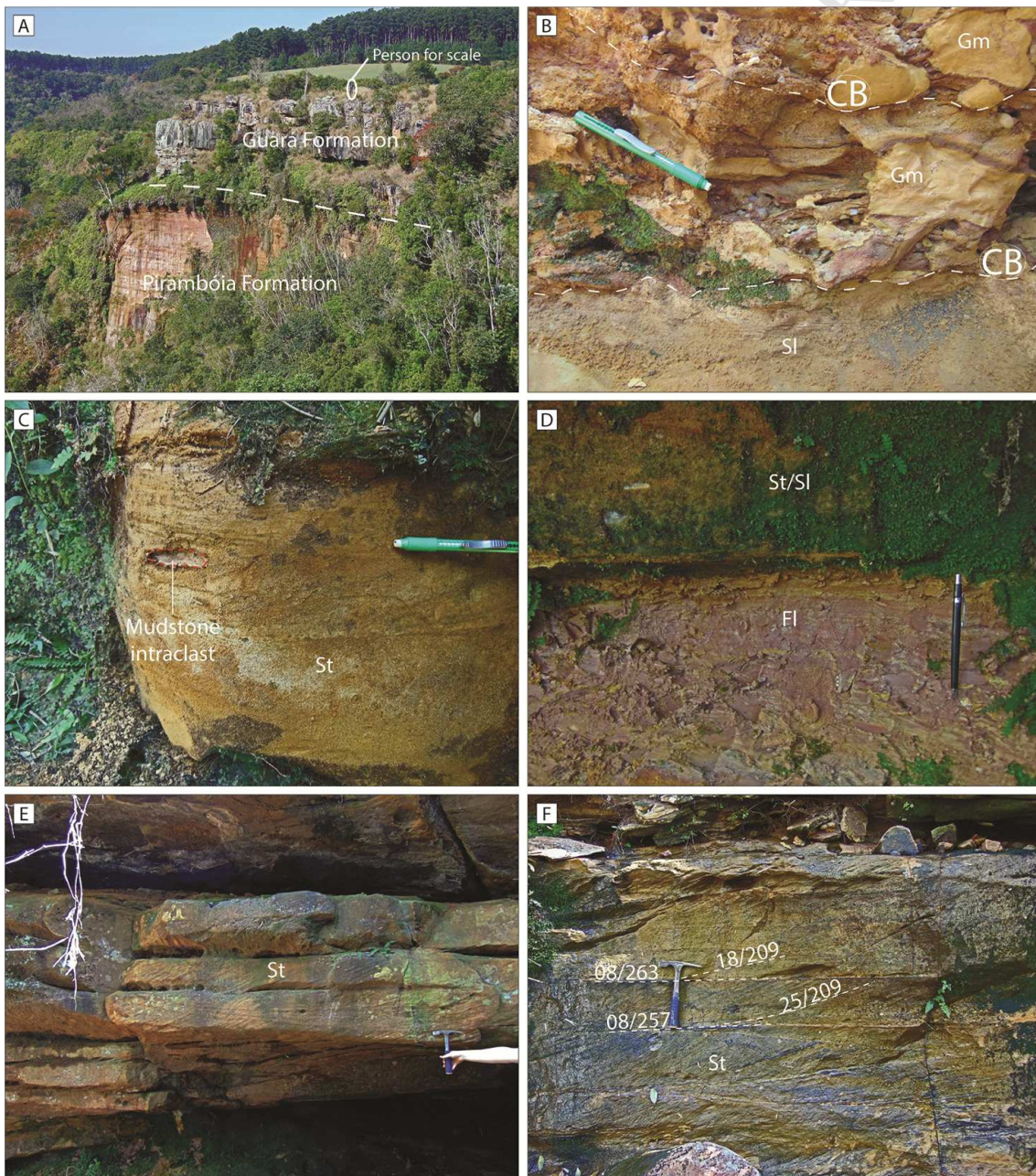
333 Paleocurrent measurements are concentrated in southwestern quadrant (Fig. 3). The  
334 mean vectors vary from 230° to 248°. Only in Section 3 there is a deviation to south, with mean  
335 vector to azimuth 179° (Fig. 3).



336

337 **Figure 5.** Details of Section 2 (Fig. 3). A) Photo of Section 2. Amalgamated channel bodies  
 338 (thin white dashed lines) below unconformity (thick white dashed line) that separates Guará and

339 Botucatu Formations, the latter represented by a large-scale cross-stratified set of aeolian dune.  
 340 B) Normal-graded foresets that form the trough cross-stratification (facies St). C) Fine-grained  
 341 sandstone lithoclasts aligned over erosive surface and D) medium-grained sandstone lithoclast  
 342 (highlighted by the yellow dashed line), at the channel bases. E) Coset of ripples cross-  
 343 lamination (facies Sr) above cross-stratified set of subaqueous dune (facies St). F) Sharp surface  
 344 boundary (white dashed line) between fluvial deposits of Guará Formation (facies Sr) and large  
 345 scale trough cross strata of aeolian dunes of Botucatu Formation (facies St(e)). Compass for  
 346 scale over the surface = 15 cm width. G) Detail of large-scale cross stratified set (facies St(e)) of  
 347 aeolian dune, Botucatu Formation.  
 348



349

350 **Figure 6.** Details of Section 3 (Fig. 3). A) The unconformity between Pirambóia and Guará  
351 Formations, in a view of the landscape near Section 3. B) Intraformational massive  
352 conglomerates (facies Gm) over channel basal surfaces of two highly amalgamated channels.  
353 Pen length = 15 cm. C) Cross-stratified sandstone with mud clast (facies St). D) Sharp erosive  
354 surface of the channel base overlying the single floodplain mudstone (facies Fl) of the four  
355 sections studied. E) Cross-stratified isolated sets (facies St; hammer length = 28 cm). F)  
356 Composed coset (facies St) of a compound downstream accretion element (DA). The basal  
357 surfaces of the sets represent the accretion surfaces, dipping gently downstream (measures in  
358 horizontal numbers). The inclined truncated lines are the dunes foresets migrating in the front  
359 side of the bar element (paleocurrent measures in inclined numbers).

360 Interpretation

361 The fining-upward packages, the normal grading in foresets and sets, the presence of  
362 mud clasts associated with numerous erosive surfaces are characteristics of fluvial deposits  
363 (Collinson, 1996). The predominance of cross-stratified sets representing subaqueous dunes  
364 suggests perennial fluvial channels (Miall, 1996; Allen et al., 2013). The occurrence of  
365 downstream accretion elements, representing mid-channel and transverse bars migration,  
366 together with narrow dispersion of paleocurrents, points to a low sinuosity perennial fluvial  
367 system with considerable channel depth (Miall, 1996; Chakraborty, 1999; Scherer et al., 2015).  
368 The near absence of mudstones representing overbank deposits (notable in the logs of Fig. 3) in  
369 contrast with recurrence of mud clasts over erosive surfaces indicates a highly amalgamated and  
370 strongly erosive system that cannibalized overbank deposits. This amalgamation is a signal of  
371 low accommodation/supply ratio (Martinsen et al. 1999). All these characteristics indicate that  
372 Guará Formation represents highly amalgamated multistorey fluvial deposits in braided-channel  
373 belts.

374 5.3. *Botucatu Formation*

375 5.3.1. *Aeolian dune facies association*

376 Aeolian deposits of Botucatu Formation comprises fine- to medium-grained,  
377 moderately to well-sorted sandstones, with well-rounded grains. These sandstones constitute  
378 three lithofacies (Fig. 3): large scale trough cross-stratified sets (St(e); Fig 5A, F and G), large-  
379 scale planar cross-stratified sets (Sp(e)) and low-angle cross-stratification (Sl(e), Fig. 4H).

380 Cross-stratification foresets are exclusively formed by translantent subcritical wind  
381 ripples in millimetric inversely graded lamination (see facies St(e) and Sp(e) in Table 1). In the  
382 studied area, 3 to 5 cm thick massive inversely graded strata were generated by grainflow in the  
383 lee side of the dunes (Fig. 5A, F and G); or in 15 cm thick cycles alternating both wind ripples  
384 and grainflow strata. Sets from 1.5 to 6 m thick occur superimposed, bounded by planar sharp  
385 truncating surfaces, or separated by packages of low-angle cross-stratified sandstones. Dip-  
386 direction of foresets of these cross-strata shows a large dispersion between NW and SE (rose  
387 diagrams in Fig. 3). Low-angle cross-stratified sets are constituted by the migration of  
388 translantent subcritical wind ripples resulting in millimetric inversely-graded lamination (Table 1,  
389 Fig. 4H).

390 Interpretation

391 The presence of fine to medium-grained sandstones, with well-sorted and well-  
392 rounded grains arranged in cross-strata sets composed of wind ripples and grainflow strata  
393 suggest aeolian dune deposits (Hunter, 1977; Kocurek, 1981, 1991, 1996; Uličný, 2004).  
394 Trough cross stratification allied to high dispersion in the direction of curved foresets indicates  
395 crescent dunes with a sinuous crestline (e.g. 3D dunes). However, expressive sets of planar  
396 cross stratification demonstrate the occurrence of straight-crested transversal dunes (2D dunes).

397 The presence of cycles alternating grainflow strata and ripple laminae indicates the  
398 occurrence of intervals during which the dunes had well-developed slipfaces that alternated with  
399 periods during which part of the lee face was covered by wind ripples (Kocurek, 1991). This  
400 cyclic strata pattern suggests to seasonal changes in wind direction (Loope et al., 2001; Scherer  
401 and Goldberg, 2010).

402 Horizontal to low-angle stratification characterizes both sandsheet and dune-plinth  
403 deposits (Fryberger et al., 1979; Kocurek and Nielson, 1986). In relation to sandsheets, dune  
404 plinths tend to be finer-grained and are more often associated with aeolian dune cross-stratified  
405 beds (Eriksson and Simpson, 1998). Due to the homogeneity in sedimentary structures  
406 (exclusively wind-ripple lamination, Fig. 4H), the absence of sedimentary structures that  
407 character moisture during deposition in addition to the relation with aeolian dune cross-strata



408 suggest that the packages of low-angle stratification of Botucatu Formation are the record of  
409 aeolian dune plinths.

410

## 411 **6. Bounding surfaces**

412 The contact between Pirambóia and Guará Formation in Paraná State is sharp contact  
413 with regional significance (Fig. 3, Fig. 4C, Fig. 6A), marking an abrupt lithological shift from  
414 arkose and subarkose fine-grained sandstone, massive, to quartzose coarse-grained gravelly  
415 sandstone with trough cross stratification (Fig. 4C). This surface represents a change from a wet  
416 aeolian system with ephemeral fluvial influence to a perennial braided fluvial system (Fig. 3 and  
417 4).

418 The transition from Guará Formation to Botucatu Formation is a regionally-correlated  
419 sharp surface (Fig. 3, Fig. 4G, Fig 5A and F) that represents the abrupt lithological transition  
420 between quartzose, coarse-grained gravelly sandstones, trough cross-stratified and arkose, fine  
421 to medium-grained sandstones, from a braided fluvial system to a dry aeolian depositional  
422 system.

423

## 424 **7. Depositional systems**

425 The relation between aeolian dunes and aeolian sandsheets and interdunes under water  
426 table influence points to a wet aeolian system. Additionally, the influence of ephemeral fluvial  
427 deposits in aeolian sedimentation characterizes the Pirambóia Formation succession as a fluvial-  
428 wet aeolian depositional system. A similar interpretation was accomplished by Wu and  
429 Caetano-Chang (1992) and Caetano-Chang and Wu (1994) to Pirambóia Formation in São  
430 Paulo State.

431 The multistorey, unidirectional and highly erosive features of fluvial deposits of the  
432 Guará Formation indicate an amalgamated perennial braided fluvial system. The fluvial origin  
433 of Guará Formation deposits was identified in other regions of the basin (Scherer and Lavina,  
434 2005, 2006; Reis, 2016)

435 The dominance of dune deposits, without interdune preservation, indicates that the  
436 deposits of Botucatu Formation are part of a dry aeolian system. This point of view is in  
437 accordance with previous (Bigarella and Salamuni, 1961; Soares, 1975; Scherer, 2000, 2002;  
438 Scherer and Lavina, 2006).

439

## 440 **8. Discussion**

### 441 *8.1. Stratigraphic Evolution*

442 The regional stratigraphic logging and facies analysis allowed the recognition of five  
443 facies associations as part of three depositional systems, each corresponding to one independent  
444 stratigraphic unit. The units are: (i) a fluvial influenced wet aeolian depositional system in  
445 Pirambóia Formation; (ii) a perennial braided fluvial system in Guará Formation; and (iii) a dry  
446 aeolian system corresponding to Botucatu Formation.

447 Using sequence stratigraphy, large scale interpretations are limited. The volume of  
448 data recorded from Pirambóia and Botucatu Formation are not representative of their regional  
449 significance. These formations are not the main focus of this study, and although the collected  
450 data does not cover their full vertical successions, it is possible to make an evaluation of their  
451 stratigraphic evolution based on the herein described outcrops.

452 The record of Pirambóia Formation shows the interaction of aeolian dunes and  
453 interdunes or wet aeolian sandsheets with ephemeral fluvial processes. The studied succession  
454 has two portions separated by a gap of 15 m (Fig. 3, Section 1). In the first portion, a succession  
455 of cross-stratified sets of aeolian dunes is recognized, separated by low-angle to horizontally  
456 stratified strata of aeolian origin and a small subaqueous dune. The position of these  
457 horizontally stratified strata, between large scale aeolian cross strata, suggests the preservation  
458 of interdune deposits. The small scale subaqueous dunes demonstrate the invasion of interdune  
459 space by fluvial streams.

460 The second portion of Pirambóia Formation starts with 3 m of aeolian facies (low-  
461 angle strata formed by wind ripple migration and adhesion lamination), succeeded by facies of

462 fluvial origin (low-angle cross stratification, current ripples and a massive bed), with no  
463 recurrence of aeolian facies up to the boundary with Guará Formation facies (Fig. 3, Section 1).  
464 Here, the aeolian portion demonstrates an increase of humidity influencing the aeolian transport,  
465 in the transition from wind ripples to adhesion lamination (Fig. 3, Section 1, Fig. 4B). The  
466 absence of aeolian dunes covering these beds suggests that these successions record a wet  
467 aeolian sandsheet.

468           The record of Pirambóia Formation in Section 1 (Fig. 3) shows a transition from facies  
469 of dry aeolian processes (aeolian dunes and dry aeolian sandsheets) passing through aeolian  
470 facies influenced for the water table (wet aeolian sandsheet, facies Sa(e)) and ending ephemeral  
471 fluvial deposits (facies St, Sl, Sm and Sr). This vertical facies succession represents the increase  
472 in humidity in the aeolian system along time, in a wetting-upward trend. The increase in  
473 humidity induced by the rise of the phreatic water table, reduced gradually the supply of dry  
474 sand, inhibiting the aeolian dune formation until the ephemeral fluvial processes prevailed.

475           The sharp bounding surface separating the units can be classified as an unconformity,  
476 marked by abrupt facies shift between Pirambóia and Guará Formations (Fig. 3, Fig. 4C, Fig.  
477 6A), including color (from white yellowish to orange brownish), grain size (from fine- to  
478 coarse-grained), detrital composition (from arkose/subarkose to quartzarenite) and sedimentary  
479 structures (from massive to trough cross-stratified). This facies change represents an abrupt  
480 contact between ephemeral fluvial deposits of the Pirambóia Formation and multistorey fluvial  
481 channels of the Guará Formation, marking a major transition from a wet aeolian depositional  
482 system to a perennial braided fluvial system. Besides that, this surface has regional significance,  
483 correlated for nearly 100 km between Sections 1 and 3 (Fig. 3, Fig. 4C, Fig. 6A). The hiatus  
484 represented by this surface is unknown because the age of Pirambóia Formation is  
485 undetermined. The absence of pedogenic features below the unconformity may be explained by  
486 the erosive character of channelized fluvial deposits of Guará Formation, which probably  
487 caused the erosion of the superficial layer of pre-existent rocks. The presence of sandstone  
488 pebble to boulder lithoclasts concentrated over erosive surfaces in Guará Formation deposits  
489 (Fig. 4D and E, Fig. 5C and D) is diagnostic of the erosion of pre-existent consolidated

490 sedimentary rocks. By context, these lithoclasts represent the original rocks of Pirambóia  
491 Formation. If the deposits of Pirambóia Formations were consolidated by diagenesis during the  
492 activity of Guará Formation fluvial channels, then a time hiatus would be assumed between the  
493 two units.

494           The composition and texture of the sandstones of the Guará Formation – well-rounded  
495 quartzarenites – are a strong characteristic of recycled sedimentary rocks, in other words,  
496 formed by sediment eroded from previous sedimentary rocks (Garzanti, 2016). The diagenesis  
497 and re-exposure to weathering, erosion and transport processes tend to concentrate quartz, a  
498 more resistant component in relation to feldspars and metamorphic/plutonic lithoclasts  
499 (Garzanti, 2016). The presence of gravel-sized sandstone clast, especially concentrated over  
500 scouring channel basal surfaces presumes the erosion of consolidated sandstones (Fig. 4D and  
501 E, Fig. 5C and D). This hypothesis is reinforced by the location of the study area and the  
502 paleocurrent patterns to SSW which suggest sediment transport from a source area located in  
503 northeastern Paraná Basin.

504           In the four studied sections, the Guará Formation is marked by the predominance of  
505 cross strata generated by subaqueous dune migration. In three of the sections studied (sections  
506 1, 2 and 3, Fig. 3), the presence of large cross strata is notable, both simple and composed,  
507 representing downstream accretion elements (Fig. 3, 4F, 5F). These architectural elements are  
508 the typical unit of construction and migration of mid-channel fluvial bars (Miall, 1985;  
509 Wizevich, 1992; Bridge, 1993; Miall, 1996; Jo and Chough, 2001; Scherer et al., 2015). The  
510 mudstone bed (facies Fl, Fig. 3, section 3) represents overbank deposits in low energy  
511 floodplains and the recurrence of gravel-sized mud clasts over scour surfaces at the base of  
512 cross-stratified sets signal the low preservation potential of these deposits, frequently eroded by  
513 new channels (Miall, 1977; Ramos et al., 1986; Wizevich, 1992; Jo and Chough, 2001). The  
514 high number of channel boundaries (multistorey) identified in relatively thin successions,  
515 associated with low preservation of overbank deposits, is characteristic of braided rivers in the  
516 context of low vertical accommodation space (Shanley and McCabe, 1993; Wright and Marriot,  
517 1993; Martinsen et al. 1999; Scherer et al., 2015).

518 The contact between Guará and Botucatu Formations is a sharp surface (Fig. 5A),  
519 marked by an abrupt facies shift where multistorey fluvial channel deposit of a perennial  
520 braided fluvial system of Guará Formation is overlain by superimposed sets of aeolian dunes of  
521 the Botucatu Formation. The Guará-Botucatu unconformity was described in detail in southern  
522 Paraná Basin (Scherer and Lavina 2006; Amarante et al., 2019). In the Rio Grande do Sul State,  
523 Scherer and Lavina (2006) mapped this unconformity for a 170 km long outcrop belt,  
524 identifying features of time hiatus as polygonal fractures and calcrete clasts at the base of  
525 Botucatu Formation. Amarante et al. (2019) recognized the surface in northwestern Uruguay,  
526 highlighting the shift of depositional systems through it. The substantial climatic change  
527 necessary to recover a perennial river system by a hyper-arid aeolian deposit (Scherer, 2000;  
528 Scherer and Lavina, 2006, Amarante et al. 2019) is significant evidence of a sequence boundary.  
529 This change was also observed in this study in Paraná state.

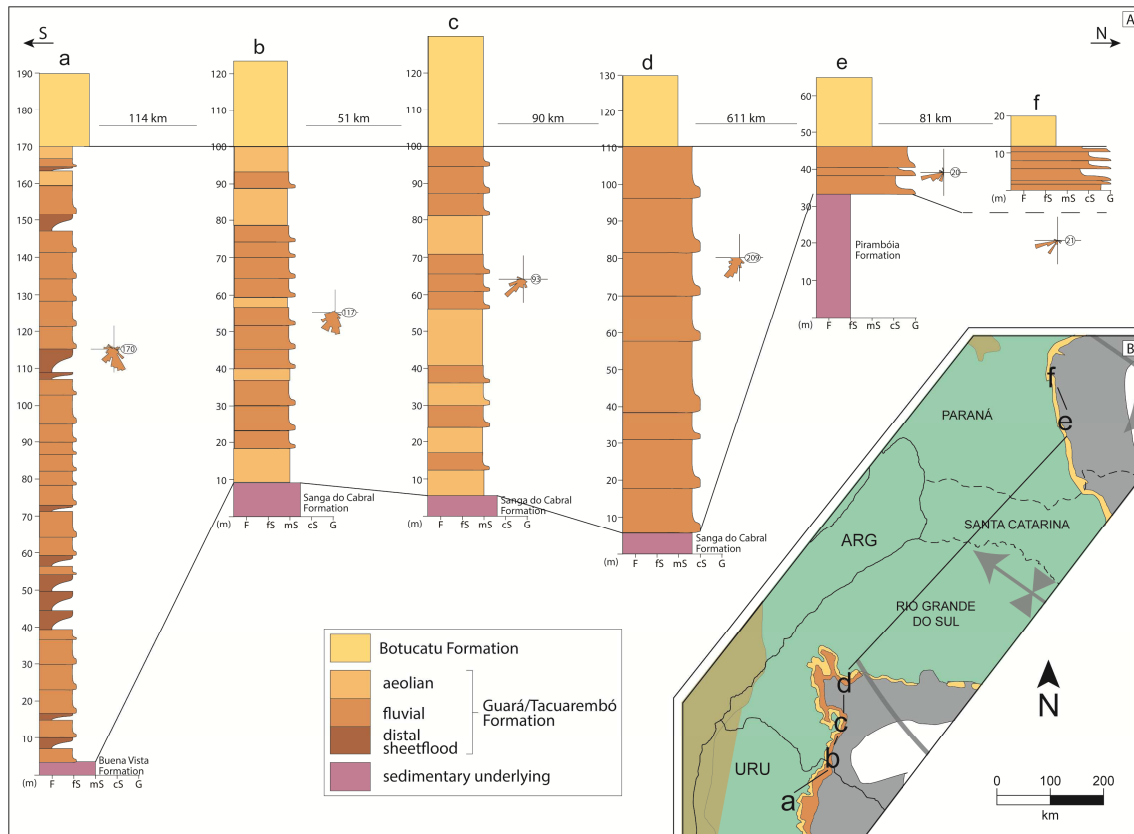
530 The time of this boundary could be supposed by relative datation. Studies about the  
531 palaeofauna and palaeoichnofauna purpose Upper Jurassic age to Guará Formation (Scherer and  
532 Lavina, 2005; Dantzien Dias et al., 2007; Perea et al., 2009). Francischini et al. (2015) point to a  
533 significant difference in the dimensions in the dinosaur palaeofaunas between Guará and  
534 Botucatu Formation, suggesting that the Botucatu aridization reduced the size of the species.  
535 The age of Botucatu Formation final deposition is directly related with volcanic floods of Serra  
536 Geral Formation, dated in Valanginian (Renne et al., 1992; Thiede and Vasconcelos, 2010;  
537 Rossetti et al., 2017). In this sense, between Upper Jurassic and Valanginian we can attribute at  
538 least 5 million years of hiatus to the Guará-Botucatu unconformity, following the International  
539 Stratigraphic Chart (Cohen et al., 2013).

540 The Botucatu Formation succession shows large scale trough cross stratified sets with  
541 thicknesses varying from 1.5 to 6 m composed by wind ripple lamination and grainflow  
542 stratification. The sets dominated by wind ripples appear to be concentrated at the base, while  
543 the grain flow strata arise late in the vertical facies succession. This indicates upward increase in  
544 dune size, permitting the development of a slipface in the lee side of the dunes (Kokurek, 1991,  
545 1996). The non-preservation of interdune deposits corroborates the interpretation of a dry

546 aeolian system for the Botucatu Formation, in which the dunes climbed each other without the  
547 formation of interdune deposits due to lack of influence of phreatic water table (Mountney,  
548 2012).

#### 549 8.2. *The Guará Formation in Gondwana context*

550 The Guará Formation's braided fluvial deposits in Paraná state represents the proximal  
551 area of a wide depositional basin. Regional correlation integrating Scherer and Lavina (2006)  
552 and Amarante (2019) shows that Guará Formation constitutes the record of continental  
553 depositional systems in an area >800 km in north-south extension (Fig. 7). The facies and facies  
554 associations distribution also shows downstream shifting in depositional systems of Guará  
555 Formation, starting with fluvial systems, grading to fluvial-aeolian and ending in fluvial  
556 ephemeral and terminal distal sheetfloods. The paleocurrent patterns are similar in all sections,  
557 preferentially to SSW (see rose diagrams in Fig. 7). There is a reduction of general grain size of  
558 the deposits to the southwest direction, following the paleocurrent trend, starting with  
559 conglomeratic sandstones and conglomerates in Paraná up to fine-grained sandstones in  
560 Uruguay. The extension, the shifting depositional system and the reduction in grain size along  
561 the paleocurrent trend reinforce the proposition of Amarante et al. (2019) that Guará and  
562 Tacuarembó Formations constitute a big distributive fluvial system, following the models  
563 purposed by Hartley et al. (2010), Weissmann et al. (2010), Owen et al. (2015) and Owen et al.  
564 (2018).



565

566 **Figure 7.** A) Regional correlation and cross-section through the Guar Formation occurrence  
 567 area between the southern portion (section a) and the central portion (section f) of Paran Basin.  
 568 Section “a” has been adapted from Amarante et al. (2019). Sections “b” and “c” from Scherer  
 569 and Lavina (2005, 2006). Section “d” from Scherer and Lavina (2006) and Reis (2016).  
 570 Sections “e” and “f” from this study. B) Indicates the location map the cross-section, as a detail  
 571 of Fig. 1B.

572

573

574

575

576

577

The Guar Formation as outlined by depositional model allows Southwestern  
 Gondwana palaeoenvironmental reconstructions. The model suggests that Paran Basin was  
 dominated by fluvial and fluvial-aeolian systems in Upper Jurassic. The paleoflow points to a  
 depocenter somewhere near the Argentina-Uruguay border, a unique condition in Paran Basin  
 history, in which the depocenter was located in the central portion of the basin. The distribution  
 of the depositional systems points to an endorheic shallow basin.

578

579

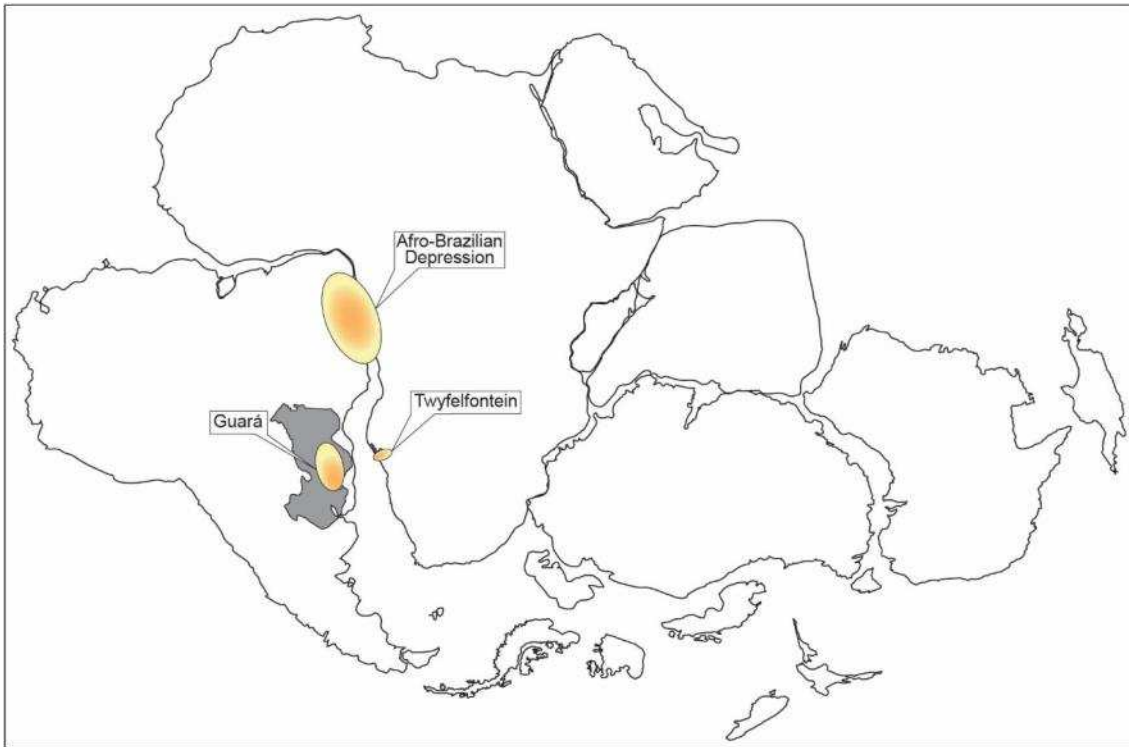
580

581

582

The basal portion of the Twyfelfontein Formation in Namibia, southern Africa, is  
 another example of an Upper Jurassic fluvial-aeolian succession (Fig. 8), designated by  
 Mountney (1998) as Khrone Member (alluvial) and Mixed Unit (fluvial-aeolian) which precedes  
 the Main Aeolian Unit (continuity of Botucatu Formation in African continent). Although the  
 stratigraphic position of the Mixed Unit is the same as Guar Formation, below the Botucatu

583 Formation, detailed studies were not done to understand the stratigraphic relation between the  
 584 units.



585  
 586 **Figure 8.** Upper Jurassic fluvial-aeolian occurrences in southwestern Gondwana: orange oval  
 587 areas indicate the estimated extension and position inside Gondwana of the systems of Afro-  
 588 Brazilian Depression, Guará Formation (Brazil) and Twyfelfontein Formation (Namibia).  
 589 Gondwana reconstruction based on Schmitt and Romeiro (2017). Grey outlined areas = Paraná  
 590 Basin and Huab Basin.

591 Similar depositional systems are found in reconstructions of Upper Jurassic Afro-  
 592 Brazilian Depression setting (Fig. 8; Kuchle et al., 2011). These authors proposed that a fluvial,  
 593 aeolian and lacustrine succession was deposited in a broad shallow endorheic basin occurring  
 594 between Northeastern Brazil and Western Africa. These records and Guará model point to the  
 595 existence of two Neo-Jurassic broad endorheic shallow basins in Gondwana (Fig. 8). Morley  
 596 (2002) proposed the Early Rift Stage as a wide shallow basin formed by the aggregation of  
 597 small slip faults in a region. This basin would occupy an area much bigger than the subsequent  
 598 rift valleys (Morley, 2002). Kuchle and Scherer (2010) proposed a stratigraphic classification to  
 599 this sedimentation: Rift Initiation Tectonic System Tract.

600 Different paleogeographic models predicted tectonism in the southwestern part of  
 601 Gondwana in pre break up stages. The palaeomagnetism based model of Seton (2012) proposed



602 transcurrent movements in the region of Chaco-Paraná around 150 Ma (Tithonian) that the  
603 authors attributed to the individualization of “Paraná subplate”. Salomon et al. (2017) analyzed  
604 the extensional structures of the conjugated margin of southern Brazil-Namibia and purposed a  
605 progressive rotation of southern South American Plate generated extension in a vast in a wide  
606 region around the future South Atlantic Rift. Is plausible to suppose that this tectonism  
607 promoted subsidence and sedimentation after the culmination of Gondwana break-up later in  
608 Lower Cretaceous.

609

## 610 **9. Conclusions**

611 The Upper Jurassic Guará Formation is recognized in the northern portion of Paraná  
612 Basin (Paraná state, Brazil). The formation records multistorey channels of a braided fluvial  
613 system. Sedimentological features and stratigraphic position allow the distinction of Guará  
614 Formation from Pirambóia and Botucatu formations (respectively underlying and overlying  
615 units). Fluvial paleocurrent pattern to SSW and detrital composition points to ancient  
616 stratigraphic units of Paraná Basin as sedimentary source area.

617 The spatial area covered by Guará Formation is thus expanded to a >800 km area with  
618 an overall north to south extension (Fig. 1, Fig. 7). This new fact points to a special geotectonic  
619 context for the Paraná Basin in Upper Jurassic, where a broad distributive fluvial system  
620 flowing from NE to SW interacted in distal portions with aeolian systems filling an endorheic  
621 basin. Fluvial-aeolian sedimentation is found in other parts of southwestern Gondwana in Upper  
622 Jurassic, as Huab Basin in Namibia and Afro-Brazilian Depression. These sedimentary  
623 successions are the record of the early stages of Gondwana break-up.

624

## 625 **10. Acknowledgements**

626 A. D. Reis thanks National Council for Scientific and Technological Development  
627 (CNPq) for the doctorate scholarship. Special thanks to Léo A. Hartmann for major suggestions  
628 and revision of manuscript, to Luiz Fernando De Ros for references and insights and to Rafael

629 Adriano for the help with graphic work. The authors are very grateful for the suggestions of  
630 three anonym reviewers.

## 631 **11. References**

632 Allen, J.R.L., 1963. The classification of cross-stratified units, with notes on their origin.  
633 *Sedimentology* 2, 93-114.

634 Allen, J.R.L., 1983. Studies in fluvial sedimentation: bars, bar complexes and sandstone  
635 sheets (low-sinuosity braided streams) in the Brownstones (Lower Devonian), Welsh  
636 Borders. *Sedimentary Geology* 33, 237-293.

637 Allen, J.P., Fielding, C.R., Rygel, M.C., Gibling, M.R., 2013. Deconvolving signals of tectonic  
638 and climatic controls from continental basins: an example from the Late Paleozoic  
639 Cumberland Basin, Atlantic Canada. *Journal of Sedimentary Research* 83, 847-872.

640 Almeida, F.F.M., Melo, C., 1981. A Bacia do Paraná e o vulcanismo mesozóico. In: Bistrichi,  
641 C.A., Carneiro, C.D.R., Dantas, A.S.L., Ponçano, W.L. (Eds.), *Mapa geológico do Estado*  
642 *de São Paulo – nota explicativa*. Instituto de Pesquisas Tecnológicas 1, 46-77.

643 Amarante, F.B., Scherer, C.M.S., Goso Aguilar, C.A., Reis, A.D., Mesa, V., Soto, M.,  
644 2019. Fluvial-eolian deposits of the Tacuarembó Formation (Norte Basin – Uruguay):  
645 Depositional models and stratigraphic succession. *Journal of South American Earth*  
646 *Sciences* 90, 355-376. Bigarella, J.J., Salamuni, R., 1961. Early Mesozoic wind patterns as  
647 suggested by dune bedding in the Botucatu sandstone of Brazil and Uruguay. *Geological*  
648 *Society of America Bulletin* 72, 1089-1106.

649 Biswas, A., 2005. Coarse aeolianites: sand sheets and zibar-interzibar facies from  
650 Mesoproterozoic Cuddapah Basin, India. *Sedimentary Geology* 174, 149-160.

651 Bridge, J.S., 1993. The interaction between channel geometry, water flow, sediment transport  
652 and deposition in braided rivers. In: Best, J.L., Bristow, C.S. (Eds.), *Braided Rivers*.  
653 *Geological Society of London Special Publication* 75, 13-72.

- 654 Bridge, J.S., Best, J.L., 1988. Flow sediment transport and bedform dynamics over the transition  
655 from upper-stage plane beds: implications for the formation of planar laminae.  
656 *Sedimentology* 35, 753-763.
- 657 Caetano-Chang, M.R., Wu, F.-T., 1994. Afloramento-modelo da Formação Pirambóia.  
658 *Geociências*, 13, 371-385.
- 659 Chakraborty, T., 1999. Reconstruction of fluvial bars from the Proterozoic Mancherl Quartzite,  
660 Pranhita–Godavari Valley, India. In: Smith, N.D., Rogers, J. (Eds.) *Fluvial*  
661 *Sedimentology VI*, International Association of Sedimentologists Special Publication 28,  
662 451-466.
- 663 Chakraborty, T., Chakraborty, C., 2001. Eolian-aqueous interactions in the development of a  
664 Proterozoic sand sheet: Shikaoda Formation, Hosangabad, India. *Journal of Sedimentary*  
665 *Research* 71, 107-117.
- 666 Clemmensen, L.B., Dam, G., 1993. Aeolian sand-sheet deposits in the Lower Cambrian Neksø  
667 Sandstone Formation, Bornholm, Denmark: sedimentary architecture and genesis.  
668 *Sedimentary Geology* 83, 71-85.
- 669 Cohen, K.M., Finney, S.C., Gibbard, P.L., Fan, J.-X., 2013 (updated). The ICS International  
670 Chronostratigraphic Chart. *Episodes* 36, 199-20
- 671 Collinson, J.D., 1996. Alluvial sediments. In: Reading, H.G. (Ed.), *Sedimentary Environments*  
672 *and Facies*, Third ed. Blackwell Publishing, Oxford, 37-82.
- 673 Eriksson, K.A., Simpson, E.L., 1998. Controls on spatial and temporal distribution of  
674 Precambrian eolianites. *Sedimentary Geology* 120, 275-294.
- 675 Francischini, H., Dentzien-Dias, P.C., Fernandes, M.A. Schultz, C.L., 2015. Dinosaur  
676 ichnofauna of the Upper Jurassic/Lower Cretaceous of the Paraná Basin (Brazil and  
677 Uruguay). *Journal of South American Earth Sciences* 63, 180-190.
- 678 Francischini H., Dentzien-Dias P., Lucas S.G., Schultz C.L., 2018. Tetrapod tracks in Permo–  
679 Triassic eolian beds of southern Brazil (Paraná Basin). *PeerJ* 6:e4764.  
680 <https://doi.org/10.7717/peerj.4764>

- 681 Garzanti, E., 2016. From static to dynamic provenance analysis—Sedimentary petrology  
682 upgraded. *Sedimentary Geology* 336, 3-13.
- 683 Giannini, P.C.F., Sawakuchi, A.O., Fernandes, L.A., Donatti, L.M., 2004. Paleoventos e  
684 Paleocorrentes Subaquosas do Sistema Depositional Pirambóia nos Estados de São Paulo  
685 e Paraná, Bacia do Paraná: estudo baseado em análise estatística de dados azimutais.  
686 *Revista Brasileira de Geociências* 34, 281-292.
- 687 Harms, J.C., Southard, J.B., Spearing, D.R., Walker, R.G., 1982. Structures and sequences in  
688 clastic rocks. *SEPM Short Course* 9, 161 p.
- 689 Hartley, A.J., Weissmann, G.S., Nichols, G.J., Warwick, G.L., 2010. Large Distributive Fluvial  
690 Systems: Characteristics, Distribution, and Controls on Development. *Journal of*  
691 *Sedimentary Research* 80, 167-183.
- 692 Haszeldine, R.S., 1983. Fluvial bars reconstructed from deep, straight channel, Upper  
693 Carboniferous coalfield of northeast England. *Journal of Sedimentary Petrology* 53,  
694 1233-1248.
- 695 Hein, F.J., Walker, R.G., 1977. Bar evolution and development of stratification in the gravelly,  
696 braided Kicking Horse River, British Columbia. *Canadian Journal of Earth Sciences* 14,  
697 562-570.
- 698 Herries, R.D., 1993. Contrasting styles of fluvial-aeolian interaction at a downwind erg margin:  
699 Jurassic Kayenta-Navajo Transition, Northeastern Arizona, USA. In: North, C.P. and  
700 Prosser, J.D. (Eds), *Characterization of Fluvial and Aeolian Reservoirs*, Geological  
701 Society of London Special Publication 73, 199-218.
- 702 Hunter, R.E., 1977. Basic types of stratification in small eolian dunes. *Sedimentology* 24, 361-  
703 387.
- 704 Hunter, R.E., Rubin, D.M., 1983. Interpreting cyclic crossbedding, with an example from the  
705 Navajo Sandstone. In: Brookfield, M.E., Ahlbrandt, T.S. (Eds.), *Developments in*  
706 *Sedimentology* 38, *Eolian Sediments and Processes*. Elsevier, New York, 429-454.

- 707 Jo, H.R., Chough, S.K., 2001. Architectural analysis of fluvial sequences in the northwestern  
708 part of Kyongsang Basin (Early Cretaceous), SE Korea. *Sedimentary Geology* 144, 307-  
709 334.
- 710 Kocurek, G., 1981. Significance of interdune deposits and bounding surfaces in aeolian dune  
711 sands. *Sedimentology* 28, 753-780.
- 712 Kocurek, G., 1991. Interpretation of ancient eolian sand dunes. *Annual Review of Earth and*  
713 *Planetary Sciences* 19, 43-75.
- 714 Kocurek, G., 1996. Desert Aeolian Systems. In: Reading, H.G. (Ed.), *Sedimentary*  
715 *Environments: Processes, Facies and Stratigraphy*. Blackwell Science, Oxford, 125-153.
- 716 Kocurek, G., Fielder, G., 1982. Adhesion structures. *Journal of Sedimentary Petrology* 51,  
717 1229-1241.
- 718 Kocurek, G., Nielson, J., 1986. Conditions favourable for the formation of warm-climate  
719 aeolian sand sheets. *Sedimentology* 33, 495-816.
- 720 Kuchle J., Scherer, C.M.S., Born, C.C., Alvarenga, R.S., Adegas, F. 2011 A contribution to  
721 regional stratigraphic correlations of the Afro-Brazilian Depression – the Dom João Stage  
722 (Brotas Group and equivalent units – Late Jurassic) in northeastern Brazilian sedimentary  
723 basins. *Journal of South American Earth Sciences* 31, 358-371.
- 724 Kuchle, J., Scherer, C.M.S., 2010. Seismic stratigraphy of rift basins: techniques, methods and  
725 its application in the Recôncavo Basin. *Boletim de Geociências da Petrobras* 18, 179-  
726 2006.
- 727 Langford, R.P., Chan, M.A., 1989. Fluvial-eolian interactions: Part II, ancient systems.  
728 *Sedimentology* 36, 1037-1051.
- 729 Loope, D.B., Rowe, C.M., Joeckel, R.M., 2001. Annual monsoon rains recorded by Jurassic  
730 dunes. *Nature* 412, 64-66.
- 731 Martinsen, O.J., Ryseth, A., Helland-Hansen, W., Flesche, H., Torkildsen, G., Idil, S., 1999.  
732 Stratigraphic base level and fluvial architecture: Ericson Sandstone (Campanian), Rock  
733 Springs Uplift, SW Wyoming, USA. *Sedimentology* 46, 235-259.

- 734 Miall, A.D., 1977. A review of the braided-river depositional environment. *Earth-Science*  
735 *Reviews* 13, 1-62.
- 736 Miall, A.D., 1978. Lithofacies types and vertical profile models in braided rivers deposits: a  
737 summary. In: Miall, A.D. (Ed.), *Fluvial Sedimentology*. Canadian Society of Petrology  
738 and Geology Memoir 5, 597-604.
- 739 Miall, A.D., 1985. Architectural-elements analysis: a new method of facies analysis applied to  
740 fluvial deposits. *Earth-Science Reviews* 22, 261-308.
- 741 Miall, A.D., 1996. *The Geology of Fluvial Deposits: Sedimentary Facies, Basin Analysis and*  
742 *Petroleum Geology*. Springer-Verlag, New York, 582 p.
- 743 Milani, E.J., 1997. Evolução tectono-estratigráfica da Bacia do Paraná e seu relacionamento  
744 com a geodinâmica fanerozóica do Gondwana Sul-Occidental. Ph.D thesis. Universidade  
745 Federal do Rio Grande do Sul.
- 746 Milani, E.J., Faccini, U.F., Scherer, C.M., Araújo, L.M., Cupertino, J.A., 1998. Sequences and  
747 Stratigraphic Hierarchy of the Paraná Basin (Ordovician to Cretaceous), Southern Brazil.  
748 *Boletim IG USP, Série Científica* 29, 125-173.
- 749 Milani, E.J., Melo, J.H.G., Souza, P.A., Fernandes, L.A., França, A.B., 2007. Bacia do Paraná.  
750 In: Milani, E.J., Rangel, H.D., Bueno, G.V., Stica, J.M., Winter, W.R., Caixeta, J.M.,  
751 Pessoa Neto, O.C. (Eds.). *Bacias Sedimentares Brasileiras – Cartas Estratigráficas*.  
752 *Boletim de Geociências da Petrobras* 15(2), 265-287.
- 753 Morley, C. K., 2002. Evolution of large normal faults: Evidence from seismic reflection data.  
754 *American Association of Petroleum Geologists. Bulletin*, Tulsa, Okla., v. 86, 961-978.
- 755 Moutney, N.P., Howell, J., Flint, S. Jerram, D., 1998. Aeolian and alluvial deposition within  
756 the Mesozoic Etjo Sandstone Formation, northwest Namibia. *Journal of African Earth*  
757 *Sciences* 27, 175-192.
- 758 Moutney, N.P., 2012. A stratigraphic model to account for complexity in aeolian dune and  
759 interdune successions. *Sedimentology* 59, 964-989.
- 760 Moutney, N.P., Jagger, A., 2004. Stratigraphic evolution of an aeolian erg margin system: the  
761 Permian Cedar Mesa Sandstone, Se Utah, USA. *Sedimentology* 51, 1-31.

- 762 Mounthey, N.P., Thompson, D.B., 2002. Stratigraphic evolution and preservation of aeolian  
763 dune and damp/wet interdune strata: an example from triassic Helsby Sandstone  
764 Formation, Cheshire Basin, UK. *Sedimentology* 49, 805-833.
- 765 Owen, A., Nichols, G.J., Hartley, A.J., Weissmann, G.S., Scuderi, L.A., 2015. Quantification of  
766 a distributive fluvial system: the Salt Wash DFS of the Morrison Formation, SW USA.  
767 *Journal of Sedimentary Research* 85, 544-561.
- 768 Owen, A., Hartley, A.J., Ebinghaus, A. Weissmann, G.S., Santos, M.G.M, 2019. Basin-scale  
769 predictive models of alluvial architecture: Constraints from the Palaeocene–Eocene,  
770 Bighorn Basin, Wyoming, USA. *Sedimentology* 66, 736-763.
- 771 Pacheco, J., 1927. Relatório elucidativo do esboço da região compreendida entre o meridiano 4º,  
772 rio Itararé e os paralelos 23º34' e 28º38'. São Paulo: Relatório da Comissão Geográfica e  
773 Geológica.
- 774 Perea, D., Soto, M., Veroslavsky, G., Martínez, S., Ubilla, M., 2009. A Late Jurassic fossil  
775 assemblage in Gondwana: Biostratigraphy and correlations of the Tacuarembó  
776 Formation, Paraná Basin, Uruguay. *Journal of South American Earth Sciences* 28, 168-  
777 179.
- 778 Quintas, M.C.L., Mantovani, M.S.M. e Zalán, P.V., 1999. Contribuição ao estudo da evolução  
779 mecânica da Bacia do Paraná. *Revista Brasileira de Geociências* 29, 217-226.
- 780 Ramos, A., Sopeña, A., Perez-Arlucea, M., 1986. Evolution of Bundsandstein fluvial  
781 sedimentation in the Northwest Iberian Ranges (Central Spain). *Journal of Sedimentary  
782 Petrology* 56, 862-875.
- 783 Reis, A.D., 2016. Análise arquitetural de depósitos fluviais da Formação Guará (Jurássico  
784 Superior-Cretáceo Inferior) na borda sudeste da Bacia do Paraná, RS, Brasil. M.Sc.  
785 dissertation, Universidade Federal do Rio Grande do Sul.
- 786 Renne, P.R., Ernesto, M., Pacca, I.G., Coe, R.S., Glen, J.M.G., Prevot, M., Perrin, M., 1992.  
787 The age of Parana flood volcanism, rifting of Gondwanaland, and the Jurassic-Cretaceous  
788 boundary. *Science* 258, 975-9979.

- 789 Rossetti, L., Lima, E.F., Waichel, B.L., Hole, M.J., Simões, M.S., Scherer, C.M.S., 2017.  
790 Lithostratigraphy and volcanology of the Serra Geral Group, Paraná-Etendeka Igneous  
791 Province in Southern Brazil: Towards a formal stratigraphical framework. *Journal of*  
792 *Volcanology and Geothermal Research* 171, 59-72.
- 793 Salomon, E., Passchier, C., Koehn, D., 2017. Asymmetric continental deformation during South  
794 Atlantic rifting along southern Brazil and Namibia. *Gondwana Research* 51, 170-176.
- 795 Scherer, C.M.S., 2000. Eolian dunes of the Botucatu Formation (Cretaceous) in Southernmost  
796 Brazil: morphology and origin. *Sedimentary Geology* 137, 63-84.
- 797 Scherer, C.M.S., 2002. Preservation of aeolian genetic units by lava flow in the Lower  
798 Cretaceous of the Paraná Basin, southern Brazil. *Sedimentology* 49, 97-116.
- 799 Scherer, C.M.S., Faccini, U.F. Lavina, E.L., 2000. Arcabouço estratigráfico do Mesozóico da  
800 Bacia do Paraná. In: Holz, M., De Ros, L.F. (Eds). *Geologia do Rio Grande do Sul*,  
801 Editora da Universidade/UFRGS, Porto Alegre. 335-354.
- 802 Scherer, C.M.S, Goldberg, K., 2007. Palaeowind patterns during the latest Jurassic-earliest  
803 Cretaceous in Gondwana: Evidence from aeolian cross-strata of the Botucatu Formation,  
804 Brazil. *Palaeogeography Palaeoclimatology Palaeoecology* 250, 89-100.
- 805 Scherer, C.M.S, Lavina, E.L.C., Dias Filho, D.C., Oliveira, F.M., Bongioiolo, D.E., Aguiar, E.S.,  
806 2007. Stratigraphy and facies architecture of the fluvial–aeolian–lacustrine Sergi  
807 Formation (Upper Jurassic), Recôncavo Basin, Brazil. *Sedimentary Geology* 194, 169-  
808 193. Scherer, C.M.S., Goldberg, K., 2010. Cyclic cross-bedding in the eolian dunes of the  
809 Sergi Formation (Upper Jurassic), Recôncavo Basin: inferences about the wind regime.  
810 *Palaeogeography Palaeoclimatology Palaeoecology* 296, 103-110.
- 811 Scherer, C.M.S., Goldberg, K., Bardola, T., 2015. Facies architecture and sequence stratigraphy  
812 of an early post-rift fluvial succession, Aptian Barbalha Formation, Araripe Basin,  
813 northeastern Brazil. *Sedimentary Geology* 322, 43-62.
- 814 Scherer, C.M.S., Lavina, E.L.C., 2005. Sedimentary cycles and facies architecture of aeolian-  
815 fluvial strata of the Upper Jurassic Guar´a Formation, southern Brazil. *Sedimentology* 52,  
816 1323-1341.



- 817 Scherer, C.M.S., Lavina, E.L.C., 2006. Stratigraphic evolution of a fluvial–eolian succession:  
818 the example of the Upper Jurassic–Lower Cretaceous Guar and Botucatu Formations,  
819 Paran Basin, Southernmost Brazil. *Gondwana Research* 9, 475-484.
- 820 Schmitt, R.S., Romeiro, M.A.T. (Coords.), 2017. Gondwana Geological Map – Pre 1<sup>st</sup> edition –  
821 November 2017. Gondwana Project.  
822 [http://www.gondwana.geologia.ufrj.br/br/?page\\_id=26](http://www.gondwana.geologia.ufrj.br/br/?page_id=26)
- 823 Shanley, K.W. and McCabe, P.J., 1993. Alluvial architecture in a sequence stratigraphic  
824 framework: a case history from the Upper Cretaceous of southern Utah, USA. In: Flint,  
825 S.S., Bryant, I.D. (Eds.), *The geological modeling of hydrocarbon reservoirs and outcrop*  
826 *analogues*. International Association of Sedimentologists Special Publication 15, 21-58.
- 827 Soares, P.C. 1975. Diviso estratigrfica do Mesozico no estado de So Paulo. *Revista*  
828 *Brasileira de Geocincias* 5, 229-251.
- 829 Soares, P.C., Sinelli, O., Penalva, F., Wernick, E., Souza, A. Castro, P.R.M., 1973. Geologia do  
830 nordeste do Estado de So Paulo. In: *Anais do XXVII Congresso Brasileiro de Geologia*,  
831 Aracaj, 209-228.
- 832 Soares, A.P., Soares, P.C., Holz, M., 2008. Correlaes estratigrficas conflitantes no limite  
833 Permo-Trissico no sul da Bacia do Paran: o contato entre duas sequncias e implicaes  
834 na configurao espacial do Aqufero Guarani. *Pesquisas em Geocincias* 35, 115-133.
- 835 Stanistreet, I.G., Stollhoffen, H., 1999. Onshore equivalents of main Kudu gas reservoir in  
836 Namibia. In: Cameron, N.D., Bate, R.H., Clure, V.E. (Eds.), *The Oil and Gas Habitats of*  
837 *the South Atlantic*. Special Publication 153. Geological Society, London, 345-365.
- 838 Thiede, D., Vasconcelos, P., 2010. Paran flood basalts: rapid extrusion hypothesis confirmed  
839 by new 40Ar/39Ar results. *Geology* 38, n. 8, 747-750.
- 840 Todd, S.P., 1989. Stream-driven, high density gravelly traction carpets: possible deposits in the  
841 Trabeg Conglomerate Formation, SW Ireland and theoretical considerations of their  
842 origin. *Sedimentology* 36, 513-530.
- 843 Turner, P., 1980. Continental red beds. *Developments in Sedimentology* 29. Elsevier,  
844 Amsterdam, 562 p.

- 845 Trewin, N.H., 1993. Controls on fluvial deposition in mixed fluvial and aeolian facies within the  
846 Tumblagooda Sandstone (Late Silurian) of Western-Australia. *Sedimentary Geology* 85,  
847 387-400.
- 848 Uličný, D., 2004. A drying-upward aeolian system of the Bohdasín Formation (Early Triassic),  
849 Sudetes of NE Czech Republic: record of seasonality and long-term palaeoclimate  
850 change. *Sedimentary Geology* 167, 17-39.
- 851 Veiga, G.D., Spalletti, L.A., Flint, S., 2002. Aeolian/fluvial interactions and high-resolution  
852 sequence stratigraphy of a non-marine lowstand wedge: the Avilé Member of the Agrio  
853 Formation (Lower Cretaceous), central Neuquén Basin, Argentina. *Sedimentology* 49,  
854 1001-1020.
- 855 Waichel, B., Scherer, C., Frank, H., 2008. Basaltic lava flows covering active aeolian dunes in  
856 the Paraná Basin in southern Brazil: features and emplacement aspects. *Journal of*  
857 *Volcanology and Geothermal Research* 171, 59-72.
- 858 Walker, R.G., 1992. Facies, facies models and modern stratigraphic concepts. In: Walker, R.G.,  
859 James, N.P. (Eds.), *Facies Models - In response to Sea Level Change*, 1-14.
- 860 Weissmann, G.S., Hartley, A.J., Nichols, G.J., Scuderi, L.A., Olson, M., Buehler, H. e Banteah,  
861 R., 2010. Fluvial form in modern continental sedimentary basins: Distributive fluvial  
862 systems. *Geology* 38, 39-42.
- 863 Wright, V.P. Marriott, S.B., 1993. The sequence stratigraphy of fluvial depositional systems:  
864 the role of floodplain sediment storage. *Sedimentary Geology* 86, 203-210.
- 865 Wizevich, M.C., 1992. Sedimentology of Pennsylvanian quartzose sandstones of the Lee  
866 Formation, central Appalachian Basin: fluvial interpretation based on lateral profile  
867 analysis. *Sedimentary Geology* 78, 1-47.
- 868 Wu, F.-T., Caetano-Chang, M.R., 1992. Estudo mineralógico dos arenitos das formações  
869 Pirambóia e Botucatu no Centro-Leste do Estado de São Paulo. *Revista do Instituto*  
870 *Geológico* 13, 58-68.

- 871 Zalán, P.V., Wolff, S., Conceição, J.C.J., Astolfi, M.A.M, Vieira, I.S., Appi, V.T., Zanotto,  
872 O.A., 1987. Tectônica e sedimentação da Bacia do Paraná. In: Atas do Simpósio Sul-  
873 Brasileiro de Geologia, 441-477.
- 874 Zerfass, H., Chemale, F. Lavina, E., 2005. Tectonic control of the Triassic Santa Maria  
875 supersequence of the Paraná Basin, southernmost Brazil, and its correlation to the  
876 Waterberg Basin, Namibia. *Gondwana Research* 8, 163-176.
- 877 Zerfass, H., Chemale, F., Schultz, C.L. Lavina, E., 2004. Tectonics and sedimentation in  
878 Southern South America during Triassic. *Sedimentary Geology* 166, 265-292.
- 879 Zerfass, H., Lavina, E.L., Schultz, C.L., Garcia, A.J.V., Faccini, U.F., Chemale, F., 2003.  
880 Sequence stratigraphy of continental Triassic strata of Southernmost Brazil: A  
881 contribution to Southwestern Gondwana palaeogeography and palaeoclimate.  
882 *Sedimentary Geology* 161, 85-105.

**Highlights**

- The area of Guará Formation (Upper Jurassic) is expanded to the central part of Paraná Basin.
- The Guará Formation is correlated in >800 km long dip section through southern Brazil and northwestern Uruguay.
- Decreasing in grain size and changes in depositional systems along the section point to a big distributive fluvial system with aeolian influence.
- The Guará Formation is the record of a wide endorheic basin related with the first tectonic efforts of Gondwana break-up